EJN European Journal of Neuroscience

FENS Federation of European Neuroscience Societies

European Journal of Neuroscience, Vol. 41, pp. 1276–1293, 2015 doi:10.1111/ejn.12874

NEUROSYSTEMS

Anatomically structured burst spiking of thalamic reticular nucleus cells: implications for distinct modulations of sensory processing in lemniscal and non-lemniscal thalamocortical loop circuitries

Akihisa Kimura and Hiroki Imbe
Department of Physiology, Wakayama Medical University, Wakayama Kimiidera 811-1, 641-8509 Wakayama, Japan

Keywords: auditory input, juxtacellular labeling, rat, topography, unit discharge

Abstract

The thalamic reticular nucleus (TRN) occupies a highly strategic position to modulate sensory processing in the thalamocortical loop circuitries. It has been shown that TRN visual cells projecting to first- and higher-order thalamic nuclei have distinct levels of burst spiking, suggesting the possibility that the TRN exerts differential influences on information processing in first- and higher-order thalamic nuclei that compose the lemniscal and non-lemniscal sensory systems, respectively. To determine whether this possibility could extend across sensory modalities, the present study examined activities of TRN auditory cells projecting to the ventral and dorsal divisions (first- and higher-order auditory thalamic nuclei) of the medial geniculate nucleus (TRN-MGV and TRN-MGD cells) in anesthetized rats, using juxta-cellular recording and labeling techniques. Burst spiking of TRN-MGV cells consisted of larger numbers of spikes with shorter inter-spike intervals as compared with that of TRN-MGD cells in auditory response evoked by noise burst stimuli. Similar distinctions, although not statistically significant, were observed in spontaneous activity. Furthermore, the features of burst spiking varied in association with the topographies of cell body and terminal field locations. These features of burst spiking are similar to those observed in the two types of TRN visual cells. First- and higher-order thalamic nuclei are known to have distinct levels of burst spiking across sensory modalities. Taken together, it is suggested that the distinctions in burst spiking in the TRN, in conjunction with those in thalamic nuclei, could constitute distinct circuitries for lemniscal and non-lemniscal sensory processing in the thalamocortical loop.

Introduction

Burst spiking has a large impact on post-synaptic cell activity (Swadlow & Gusev, 2001). Therefore, neural circuitries with distinct levels of burst spiking could operate in different manners for distinct functions. There are distinctions in the level of burst spiking between first- and higher-order thalamic nuclei that compose the lemniscal and non-lemniscal sensory systems, respectively. Thalamic cells in higher-order nuclei have higher propensities to discharge in burst as compared with those in first-order nuclei (He & Hu, 2002; Ramcharan *et al.*, 2005; Wei *et al.*, 2011). This difference could be related to the following distinct functions of thalamic nuclei: first-order nuclei, being connected with the primary sensory areas in the cortex, are primarily dedicated to uni-modal sensory processing and relay peripheral sensory inputs to the cortex, while higher-order nuclei, receiving highly processed cortical and subcortical inputs rather than peripheral uni-modal sensory inputs, serve multi-modal sensory processing (Komura *et al.*, 2001; Cappe *et al.*, 2009) and compose cortico-thalamo-cortical pathways as well (Sherman, 2012). Cell activities in these thalamic nuclei are under a significant influence of GABAergic input from the thalamic reticular nucleus (TRN) (Kim *et al.*, 1997; Yu *et al.*, 2009; Halassa *et al.*, 2011) that comprises the two types of cells projecting to first- and higher-order thalamic nuclei (Pinault, 2004). It has been shown that TRN visual cells projecting to the dorsal lateral geniculate (DLG) and lateral posterior (LP) nuclei (first- and higher-order nuclei) have high and low levels of burst spiking, respectively (Kimura *et al.*, 2012b). This contrasts with low and high levels of burst spiking in first- and higher-order thalamic nuclei. The TRN, receiving inputs from thalamic nuclei and cortical areas, plays a crucial role in gain and/or gate control of information processing in the thalamocortical loop circuitries. Therefore, the synergy between TRN and thalamic cell activities with their contrasting features of burst spiking may compose distinct information processing and attentional gating functions in the lemniscal and non-lemniscal sensory systems.

Distinctions in burst spiking between first- and higher-order thalamic nuclei are observed across sensory modalities. Analysis of burst spiking in the TRN is limited to visual modality. This raises the question of whether distinctions in burst spiking are recognizable in TRN cells of another sensory modality. To address this question, the present study examined activities of TRN auditory cells, focusing on the

Correspondence: Dr A. Kimura, as above.
E-mail: akimura@wakayama-med.ac.jp

Received 25 September 2014, accepted 11 February 2015

features of burst spiking and the targets of axonal projection. Experiments were performed on anesthetized rats and data were obtained from the two types of auditory cells projecting to first- and higher-order auditory thalamic nuclei. The results indicated not only distinctions in burst spiking between the two types of auditory cells but also variations of burst spiking related to the topographies of cell body and terminal field locations. These features of burst spiking are similar to those observed in visual cells (Kimura *et al.*, 2012b). Burst spiking of TRN cells is anatomically structured in a similar manner across sensory modalities to exert differential controls over information processing in the lemniscal and non-lemniscal sensory systems.

Materials and methods

Animals and surgical preparation

Experiments were performed on 40 adult male Wistar rats (Kiwa Laboratory Animal, Wakayama, Japan) weighing 270–355 g (mean, 325 g). All studies were carried out in accordance with the approved institutional animal care and use protocol of the Animal Research Committee of Wakayama Medical University. All experiments conformed to the National Institutes of Health Guide for the Care and Use of Laboratory Animals and the guidelines on the ethical use of animals of the Japanese Government Notification.

Animals received an initial intraperitoneal (i.p.) bolus injection of pentobarbital (5–8 mg/100 g body weight). This was followed by continuous injections of chloral hydrate (4–6 mg/100 g body weight/h, i.p.) and pentobarbital (0.5–0.8 mg/100 g body weight/h, i.p.) through a cannula placed in the abdomen, using a microinjection pump (CFV-2100; Nihon Kohden, Tokyo, Japan) to avoid supplemental bolus injections and minimize fluctuations of anesthetic levels. The animals were maintained in an areflexic state throughout the experiment. The animals were mounted on a stereotaxic apparatus. To avoid damage to the tympanic membrane, hollow ear bars with blunted tips were used. The cisterna magna was incised to reduce edema and pulsations of the brain. A local anesthetic (2% xylocaine) was infiltrated in all surgical wounds.

A burr hole was made in the skull and dura (anteroposterior, 2.5–5.0 mm posterior to bregma; mediolateral, 2.4–4.6 mm lateral to midline). This allowed access to the TRN by a vertical insertion of glass capillary into the brain for recording unit discharges and injecting biocytin (Sigma, Saint Louis, MO, USA) or neurobiotin (Vector Laboratories, Burlingame, CA, USA). A glass capillary (tip diameter, ~2.5 μm; impedance, 7–21 MΩ) was filled with 2–5% biocytin or neurobiotin dissolved in 0.5 M saline.

Stimulation and recording

Noise bursts (white noise; intensity, 70-dB SPL at the ear; duration, 100 ms including 5-ms rise and fall time) were digitally generated (100 kHz) and converted to analog voltage signals (PCI-MIO-16XE-10; National Instruments, Austin, TX, USA) and delivered from a free-field speaker (SRS-A41; Sony, Tokyo, Japan) placed lateral to the ear contralateral to the recording site. A glass capillary was vertically advanced from the cortical surface to the TRN with a micro-step driver (PC-5N; Narishige, Tokyo, Japan), monitoring neural responses to sound. Recordings were amplified (× 10 000), filtered (300–2000 Hz), digitized (20 kHz) through an A-D converter (PCI-MIO-16XE-10; National Instruments) and stored on a computer for data analysis using custom-made programs (LabVIEW; National Instruments). When juxtacellularly recorded large unit discharges (> 0.5 mV) responding to sound were obtained, a series of 20–100 noise burst stimuli (inter-stimulus interval, 2–3 s) were delivered to record the unit discharges for data analysis. Recording time was 1000 ms per stimulus, including a 0- to 200-ms pre-stimulus recording time. In a subset of cases spontaneous unit discharges were recorded for 3 min in a state with a steady ambient noise level (≤ 51 dB). Sound intensity was measured using a 1/4-inch condenser microphone (Type 4939; Brüel and Kjaer, Tokyo, Japan). At the end of recording, biocytin or neurobiotin was injected by delivering anodal current (3–23 nA, 200 ms on and 200 ms off) for 2–20 min (Pinault, 1996). Following completion of injection, the capillary was removed and the wound was closed. The animals were given post-operative care.

Histology

After a survival period of 3–6 h, the animals were deeply anesthetized with an overdose of pentobarbital (150 mg/kg body weight, i.p.) and transcardially perfused with 300 mL of 0.9% saline containing heparin (300 IU), followed by 300 mL of 4% paraformaldehyde and 0.1–0.3% glutaraldehyde in 0.1 M sodium phosphate buffer (PB, pH 7.4). Brains were removed from the skull and post-fixed overnight in the same fixative. After storage at 4 °C in 30% sucrose, 0.1 M PB for 3–4 days, the frozen brains were cut at a thickness of 70 μm in the coronal plane with a freezing microtome. The sections were incubated in 1.5% H_2O_2 in 10 mM PB and saline (PBS) for 1 h to suppress endogenous peroxidase activity. All sections were then incubated in 10 mM PBS containing avidin–biotin–peroxidase complex (ABC Elite; Vector Laboratories) and 0.5% Triton X-100 at room temperature for 4 h (Horikawa & Armstrong, 1988). After bathing in 0.1 M Tris buffer (pH 7.4) containing 0.5% cobalt acetate for 10 min, the sections were processed with 0.04% diaminobenzidine tetrahydrochloride (DAB) (Sigma), 0.015% H_2O_2 and ammonium nickel sulfate in 0.1 M Tris buffer at room temperature for 15–20 min to visualize labeling. The sections were then washed twice for 10 min in distilled water.

The sections were mounted on gelatin-coated glass slides and every fourth section was stained with neutral red. Labeling was observed under a light microscope (BX41; Olympus, Tokyo, Japan) and drawn with the aide of a camera lucida. Digital images were acquired at 40 × (numerical aperture, 0.10) or 200 × (numerical aperture, 0.40) through a CCD camera with 1.4 million pixels (HC-300Z; Fujifilm, Tokyo, Japan) attached to the microscope and stored on a computer. The drawings and images were analysed and prepared for publication using Canvas (Deneba Software, Miami, FL, USA) and Adobe Photoshop (Adobe Systems, Tokyo, Japan). The parcellation and nomenclature of the thalamic nuclei followed those of Paxinos & Watson (1997).

Data analysis

Auditory response and spontaneous activity included single spikes and trains of spikes (bursts) that appeared repetitively in the majority of recordings. Features of auditory response and spontaneous activity were analysed with regard to the numbers (per second in a post-stimulus recording of auditory response and per second in the whole recording of spontaneous activity) of all discharge events (single spikes and bursts) and all spikes (single spikes and spikes in bursts), the incidence (%) of burst spiking in the all discharge events, the number of spikes composing a burst, and the averaged and first inter-spike intervals (ISIs) of spikes in a burst. Additionally, the minimum peak response latency of discharge was measured in primary auditory response and autocorrelation function of spikes was calculated in spontaneous activity. Unit discharges evoked with latencies

< 100 ms (duration of sound stimulation) were defined as primary response that is considered to represent cell activity (onset response) directly driven by auditory input (Kimura, 2014). Late (≥ 100 ms) response repeatedly evoked after the end of sound stimulation was designated as non-primary response. Burst was defined as a train of spikes with ISIs that do not exceed 10 ms (Shosaku *et al.*, 1989; Sumitomo *et al.*, 1989; Hartings *et al.*, 2003; Llinás & Steriade, 2006; Kimura *et al.*, 2012b). Bursts isolated solely based on the maximum ISI are considered to include bursts generated on low-threshold calcium spike (LTS) (LTS bursts) and high-frequency trains of single spikes (Lu *et al.*, 1992). Putative LTS bursts were then isolated as those that were preceded by periods (≥ 100 ms) of quiescence of discharge (Lu *et al.*, 1992; Ramcharan *et al.*, 2005; Llinás & Steriade, 2006). As clusters of spiking with longer ISIs (mostly < 20 ms) and shorter preceding periods (mostly ≥ 50 ms) of quiescence discharge were observed in a subset of cases, as has been documented in previous studies (Domich *et al.*, 1986; Shosaku *et al.*, 1989; Sumitomo *et al.*, 1989), data analysis was also performed, isolating bursts with ISIs < 20 ms and putative LTS bursts with preceding quiescent periods (QPs) ≥ 50 ms. Data are expressed as the mean ± SD. Comparisons of data were performed using Student's *t*-test. Bonferonni adjustment was applied to multiple comparisons in the datasets of the incidences of event and spike, the features (the percentage of burst spiking in discharge events, the number of spikes composing a burst, and the averaged and first ISIs in a burst) of burst spiking, the spike widths and the locations of cell bodies and terminal fields, and multiple correlations in the topographies of axonal projections and the properties of burst spiking associated with the two- and three-dimensional locations of cell bodies and terminal fields. *P* values are expressed as corrected values. Difference was considered significant when corrected *P* values were < 0.05.

The locations of labeled cell bodies and terminal fields were examined to determine the topography of axonal projections of labeled cells and the relationships between the features of cell activity and the locations of labeled cell bodies and terminal fields. The location of a labeled cell along the rostrocaudal neural axis was defined as the distance (mm) from bregma of a coronal tissue section containing the labeled cell. The dorsoventral location of a labeled cell in the coronal plane of the TRN was expressed as the ratio (D-V) of the distance (a) from the most lateral edge of the TRN to the whole length (b) of the dorsal or ventral blade of the part of the TRN that contained the labeled cell (see left inset in Fig. 7A). Labeled cells were further classified into two types, those located in the lateral and medial sides (tiers) of the midline of the TRN. When it was difficult to determine the location of a labeled cell, the case was defined as a cell located in the middle part. The location of a terminal field in the ventral (MGV) or dorsal division (MGD) of the medial geniculate nucleus along the rostrocaudal neural axis was defined as the distance (mm) from bregma of a coronal tissue section containing the densest labeling. To determine the location of a terminal field in the coronal plane of the MGV, the distance of the terminal field (the center of labeling) from the dorsal or medial boundary of the MGV was measured. The two-dimensional location of the terminal field was then expressed as the ratio of the distance to the whole dorsoventral or mediolateral span of the MGV (Kimura *et al.*, 2007).

Results

Data analysis was based on 48 juxtacellularlly recorded TRN cells that responded to noise burst stimuli and sent axonal projections terminating in the MGV (TRN-MGV cell, $n = 26$) or MGD (TRN-MGD cell, $n = 22$). A case in which a cell body was not identified but a labeled terminal field was clearly observed in the MGV was included in the TRN-MGV cell group. Spontaneous activity was further recorded in a subset of cases (12 TRN-MGV and 13 TRN-MGD cells). Auditory response and spontaneous activity were analysed for comparisons between TRN-MGV and TRN-MGD cell groups, focusing on the features of burst spiking.

Representative TRN-MGV and TRN-MGD cells

A cell (case 011613-5) located in the lateral tier of the ventral sector of the TRN at 3.75 mm posterior to bregma (Fig. 1A) sent an axonal projection terminating in the ventromedial part of the MGV at 5.55 mm posterior to bregma (Figs 1A and 3A). Noise burst stimuli elicited clusters of unit discharges that appeared approximately three to five times in an 850-ms post-stimulus recording (recording trace and raster in Fig. 1A). The minimum peak response latency of unit discharges was 10.93 ms. Oscillatory activation observed in auditory response was not apparent in spontaneous activity (autocorrelation function in Fig. 1B). The incidences of single spikes and bursts were analysed in all discharge events (cyan bars in the two bar graphs of Fig. 1C) and discharge events with preceding QPs ≥ 100 ms (magenta bars). The major component of discharge events was burst spiking and the numbers of spikes composing a burst mostly ranged between six and ten in the two types of discharge events.

A cell (case 031512-8) located in the medial tier of the TRN at 4.0 mm posterior to bregma (Fig. 2A) sent an axonal projection terminating in the middle part of the MGD at 5.29 mm posterior to bregma (Figs 2A and 3B). This cell was also activated repeatedly by noise burst stimuli (recording trace and raster in Fig. 2A). The minimum peak response latency of unit discharges was 18.89 ms. Oscillatory activity was not observed in spontaneous activity (autocorrelation function in Fig. 2B). In contrast to the dominance of burst spiking in case 011613-5 (Fig. 1C), the major component of discharge events was single spikes (bar graphs in Fig. 2C). The numbers of spikes composing a burst mostly ranged between four and eight. ISIs (magnified recording trace in Fig. 2A) were longer than those observed in case 011613-5 (magnified recording trace in Fig. 1A).

ISI (inter-spike intervals to preceding and subsequent spikes designated here as 'ISIs Before' and 'ISIs After', respectively) plots (Fig. 4A) were made from recordings of auditory response (white circles) and spontaneous activity (blue circles). Additionally, 'ISIs After' of the first spikes in auditory responses were plotted (red circles) together with their response latencies that were used as abscissa values instead of 'ISIs Before'. In case 011613-5 (TRN-MGV cell) there was a cluster of plots indicating bursts preceded by QPs (ISIs Before) ≥ 100 ms in both auditory response and spontaneous activity. 'ISIs After' were all < 10 ms when 'ISIs Before' were ≥ 100 ms. In case 031512-8 (TRN-MGD cell) the 'ISIs Before' (QPs) of a comparable cluster of plots were relatively short and some of them were < 100 ms. The comparable 'ISIs After' were relatively long and some of them exceeded 10 ms. These features of ISI were generally observed in the TRN-MGV and TRN-MGD cell groups, respectively. A discrete cluster of plots with 'ISIs Before' ≥ 100 ms and 'ISIs After' < 10 ms was observed in 21 out of 26 TRN-MGV cells and seven out of 22 TRN-MGD cells.

LTS bursts of TRN cells are characterized by preceding QPs and the following peculiar pattern of ISIs in a burst (intra-burst ISI): an initial progressive decrease in ISI followed by a progressive increase in ISI (Domich *et al.*, 1986; Hartings *et al.*, 2003; Llinás &

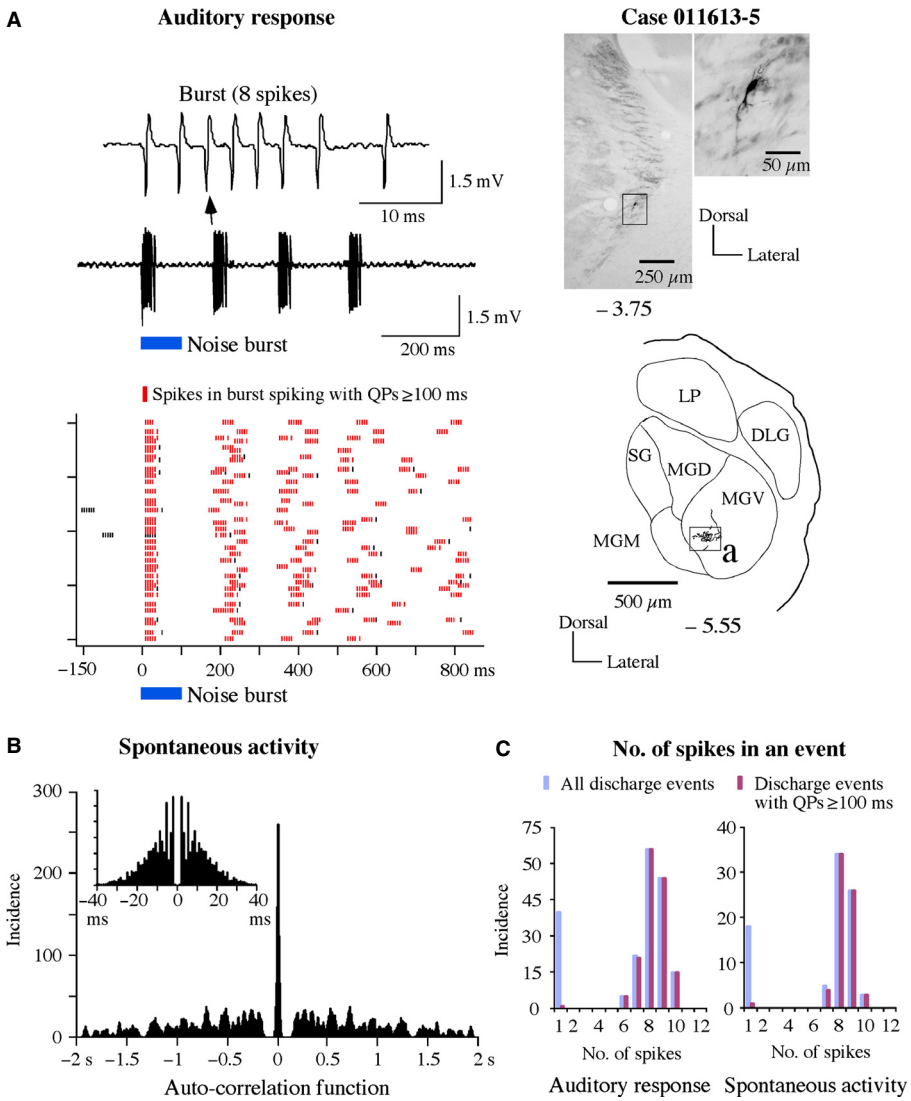

FIG. 1. Representative TRN cell projecting to the MGV. A cell located in the lateral tier of the ventral sector of the TRN (photomicrographs) projecting to the MGV (traces) exhibited mostly bursts in response to noise burst stimuli (raw trace and raster in A). Oscillatory activation was not observed in spontaneous activity (autocorrelation function in B). Red dots in the raster (A) indicate spikes in bursts with preceding QPs ≥ 100 ms. Other bursts including those observed before sound stimulation, together with single spikes, are shown as black dots. In both auditory response and spontaneous activity (bar graphs in C), the major component of discharge events was burst spiking in all discharge events (cyan bars) and events with preceding QPs (ISI Before) ≥ 100 ms (magenta bars). The ordinate of the bar graph indicates total numbers of events. The boxed area (a) in traces is magnified in Fig. 3A. The numbers below photomicrograph and trace indicate distances (mm) from bregma. MGM, medial division of the medial geniculate nucleus; SG, suprageniculate nucleus.

Steriade, 2006). The relationship between the order and length of ISIs in a burst (Fig. 4B) indicated the peculiar pattern (magnified recording traces in Figs 1A and 2A) in the most frequently observed bursts with preceding QPs ≥ 100 ms in auditory response and spontaneous activity (black and blue lines in the two upper graphs in Fig. 4B). The first bursts elicited within 100 ms after the onset of noise burst stimuli also exhibited the same peculiar pattern (red lines). The peculiar pattern was recognized irrespective of the number of spikes composing a burst in both auditory response (data not shown) and spontaneous activity (two lower graphs in Fig. 4B). On the basis of these findings, the bursts with preceding QPs ≥ 100 ms were considered to be LTS bursts (Llinás & Steriade, 2006). The peculiar pattern was observed in 25 out of 26 TRN-MGV and 20 out of 22 TRN-MGD cells. In the other three cells, first ISIs were shorter than second ISIs in both auditory response and spontaneous activity.

Distinctions in the features of auditory response and spontaneous activity between TRN-MGV and TRN-MGD cell groups

In the whole auditory response (primary and non-primary responses) (Table 1), the number of all spikes elicited by a noise burst stimulus in the TRN-MGV cell group was larger (t_{46} = 3.87, P = 0.0007) than that in the TRN-MGD cell group (ordinate values in Fig. 5A), while there was no significant difference (t_{46} = 0.77, P = 0.8863) in the number of all discharge events between the TRN-MGV and TRN-MGD cell groups (abscissa values in Fig. 5A). The difference in the number of all spikes was ascribed to a higher (t_{46} = 3.17, P = 0.0107) incidence of burst spiking and a larger (t_{46} = 4.30, P = 0.0004) number of spikes composing a burst in the TRN-MGV cell group as compared with those in the TRN-MGD cell group (abscissa values in Fig. 5B). Averaged intra-burst ISI in the TRN-

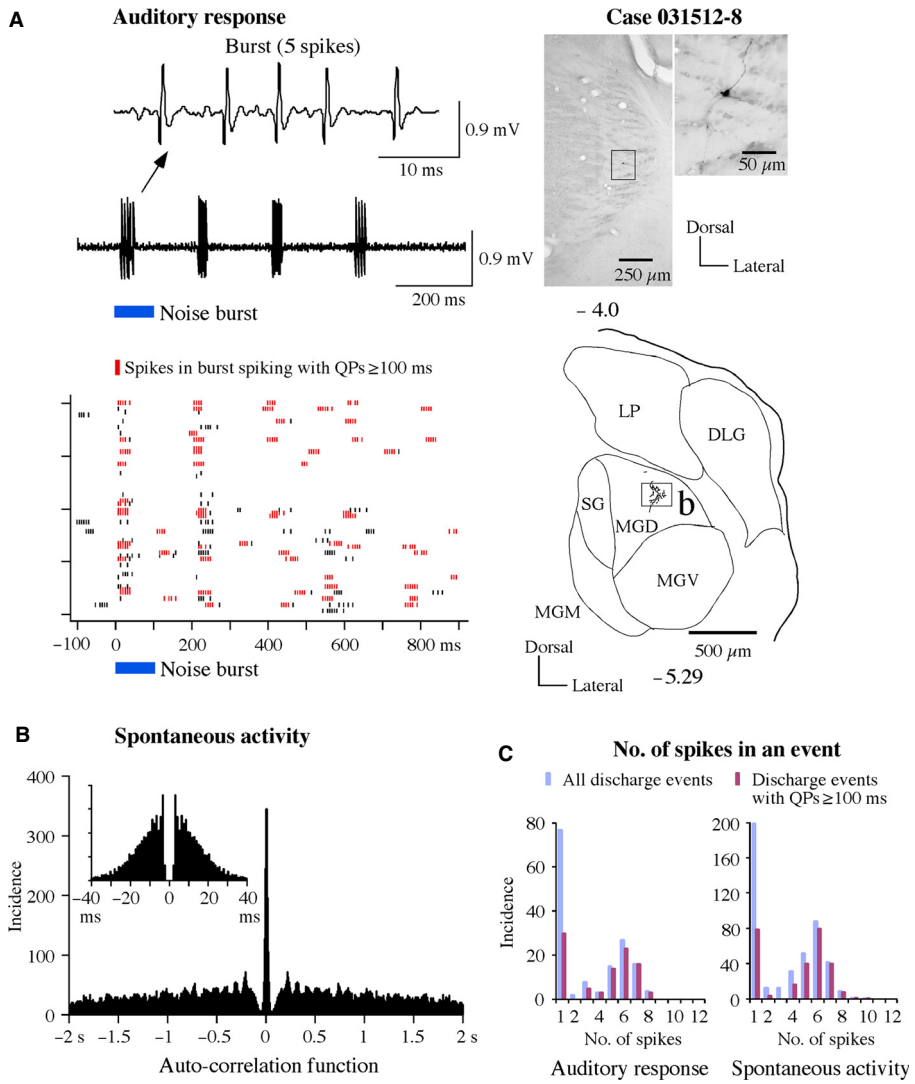

FIG. 2. Representative TRN cell projecting to the MGD. A cell located in the medial tier of the TRN (photomicrographs) projecting to the MGD (traces) exhibited frequently single spikes in auditory response (raster in A and bar graph in C) and spontaneous activity (bar graph in C). (C) The dominance of single spikes was observed in all discharge events (cyan bars) and discharge events with preceding QPs (ISI Before) ≥ 100 ms (magenta bars). Red dots in the raster (A) indicate spikes in bursts with preceding QPs ≥ 100 ms. Other bursts and single spikes are shown as black dots. Oscillation was not apparent in spontaneous activity (autocorrelation function in B). The ordinate of the bar graph indicates total numbers of events. The boxed area (b) in traces is magnified in Fig. 3B. The numbers below photomicrograph and trace indicate distance (mm) from bregma. MGM, medial division of the medial geniculate nucleus; SG, suprageniculate nucleus.

MGV cell group was shorter (t_{46} = 4.51, P = 0.0002) than that in the TRN-MGD cell group (ordinate values in Fig. 5B). First intra-burst ISI in the TRN-MGV cell group was also shorter (t_{46} = 3.93, P = 0.0011) than that in the TRN-MGD cell group. Data analysis limited to discharge events with preceding QPs ≥ 100 ms in non-primary response (Table 1 and Fig. 5C) also indicated similar differences in the number of spikes (t_{46} = 3.77, P = 0.0009), the incidence of burst spiking (t_{46} = 3.67, P = 0.0025), the number of spikes composing a burst (t_{46} = 3.75, P = 0.0020) (abscissa values in Fig. 5C), and averaged (t_{46} = 4.49, P = 0.0002) (ordinate values in Fig. 5C) and first intra-burst ISIs (t_{46} = 4.25, P = 0.0004) between the TRN-MGV and TRN-MGD cell groups. In spontaneous activity (Table 2), there were no differences in the numbers of all discharge events (t_{23} = 0.87, P = 0.7914) and spikes (t_{23} = 0.27, P = 1) between the TRN-MGV and TRN-MGD cell groups (Fig. 5D). The incidence of burst spiking in the TRN-MGV cell group did not differ (t_{23} = 1.54, P = 0.5501) from that in the TRN-MGD cell group. The number of spikes composing a burst in the TRN-MGV cell group tended to be larger than that in the TRN-MGD cell group (abscissa values in Fig. 5E), and averaged (ordinate values in Fig. 5E) and first intra-burst ISIs in the TRN-MGV cell group tended to be shorter than those in the TRN-MGD cell group; however, these differences were not statistically significant (t_{23} = 2.39, 2.49 and 2.47, P = 0.1017, 0.0811 and 0.0846). In data analysis limited to discharge events with preceding QPs ≥ 100 ms (Table 2 and Fig. 5F), there were no significant differences in the numbers of discharge events (t_{23} = 0.13, P = 1) and spikes (t_{23} = 1.03, P = 0.6288), the incidence of burst spiking (t_{23} = 1.76, P = 0.3703), the number of spikes composing a burst (t_{23} = 1.80, P = 0.3391), and averaged (t_{23} = 2.28, P = 0.1278) and first intra-burst ISIs (t_{23} = 2.39, P = 0.1014) between the TRN-MGV and TRN-MGD cell groups. In summary, TRN-MGV cells had higher propensities for burst spiking and exhibited bursts of larger numbers of spikes with shorter ISIs as compared with TRN-MGD cells in

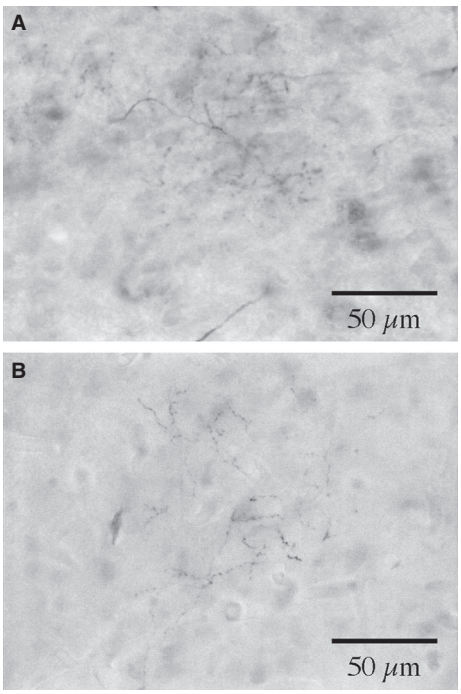

FIG. 3. Terminal fields in the MGV and MGD. TRN cells in Figs 1 and 2 sent axonal projections that formed plexuses in the MGV (A) and MGD (B), respectively.

auditory response (Table 1). Similar tendencies were observed in spontaneous activity (Table 2).

There were correlations between the numbers of all discharge events and all spikes in both auditory response (TRN-MGV cell group, $r_{24} = 0.77$, $P = 0.0002$; TRN-MGD cell group, $r_{20} = 0.51$, $P = 0.0280$; Pearson's correlation coefficient test) and spontaneous activity (TRN-MGV cell group, $r_{10} = 0.73$, $P = 0.0114$; TRN-MGD cell group, $r_{11} = 0.70$, $P = 0.0124$) (Figs 5A and D). The slope of the regression line in the TRN-MGV cell group differed from that in the TRN-MGD cell group in auditory response ($t_{44} = 2.49$, $P = 0.0166$) but not in spontaneous activity ($t_{21} = 0.93$, $P = 0.3653$). Similar correlations were observed in data analysis limited to discharge events with preceding QPs $\geq$ 100 ms in non-primary response (TRN-MGV cell group, $r_{24} = 0.87$, $P = 0.0002$; TRN-MGD-cell group, $r_{20} = 0.61$, $P = 0.0036$) and spontaneous activity (TRN-MGV cell group, $r_{10} = 0.77$, $P = 0.0046$; TRN-MGD-cell group, $r_{11} = 0.65$, $P = 0.0298$) (data not shown). The slope of the regression line in the TRN-MGV cell group also differed from that in the TRN-MGD cell group in auditory response ($t_{44} = 2.05$, $P = 0.0468$) but not in spontaneous activity ($t_{21} = 0.16$, $P = 0.8776$). With regard to the features of burst spiking in auditory response (Figs 5B and C), the numbers of spikes composing a burst in all bursts correlated with averaged intra-burst ISIs in both the TRN-MGV ($r_{24} = -0.75$, $P = 0.0004$; Pearson's correlation coefficient test) and TRN-MGD cell groups ($r_{20} = -0.73$, $P = 0.0004$): averaged intra-burst ISIs became shorter as the numbers of spikes composing a burst increased (Fig. 5B). The slope of the regression line in the TRN-MGV cell group did not differ from that in the TRN-MGD cell group ($t_{44} = 1.36$, $P = 0.1799$). The numbers of spikes composing a burst also had a similar correlation ($r_{24} = -0.50$, $P = 0.0320$) with first intra-burst ISIs in the TRN-MGV cell group but not ($r_{20} = -0.36$, $P = 0.4184$) in the TRN-MGD cell group (data not shown). In data analysis limited to burst spiking with preceding QPs $\geq$ 100 ms in non-primary response (Fig. 5C), similar correlations between the number of spikes composing a burst and averaged intra-burst ISI were observed in the TRN-MGV ($r_{24} = -0.75$, $P = 0.0004$) and TRN-MGD cell groups ($r_{20} = -0.65$, $P = 0.0032$), and there was no difference in the slope of the regression line between the TRN-MGV and TRN-MGD cell groups ($t_{44} = 0.25$, $P = 0.8051$). The numbers of spikes composing a burst also tended to correlate with first intra-burst ISIs ($r_{24} = -0.44$, $P = 0.0984$) in the TRN-MGV group (data not shown). In spontaneous activity (Figs 5E and F), the numbers of spikes composing a burst in all bursts correlated with averaged ($r_{10} = -0.90$, $P = 0.0004$) and first intra-burst ISIs ($r_{10} = -0.82$, $P = 0.0020$) only in the TRN-MGV cell group (Fig. 5E). Similar correlations (the number of spikes – averaged ISI, $r_{10} = -0.90$, $P = 0.0004$; the number of spikes – first ISI, $r_{10} = -0.81$, $P = 0.0028$) were also observed in the TRN-MGV cell group when data analysis was limited to bursts with preceding QPs $\geq$ 100 ms (Fig. 5F). In summary, the features of correlation between the numbers of discharge events and spikes differed between the TRN-MGV and TRN-MGD cell groups in auditory response (Fig. 5A) due to the higher propensities for more intense burst spiking in the TRN-MGV cell group (Table 1). This difference was not recognized in spontaneous activity (Fig. 5D). The features of correlation between the numbers and ISIs of spikes composing burst spiking were similar between the TRN-MGV and TRN-MGD cell groups in auditory response (Figs 5B and C). This similarity was not replicated in spontaneous activity (Figs 5E and F).

Spike width (combined widths of positive and negative deflections) was measured at single spikes, and the averaged and first spikes of burst spiking in spontaneous activity. There were no differences (single spike, $t_{21} = 0.09$, $P = 1$; averaged spike, $t_{23} = 0.13$, $P = 1$; first spike, $t_{23} = 0.12$, $P = 1$) in spike width between the TRN-MGV (single spike, 1.07 ± 0.26 ms; averaged spike, 1.09 ± 0.27 ms; first spike, 1.08 ± 0.26 ms) and TRN-MGD (single spike, 1.06 ± 0.15 ms; averaged spike, 1.08 ± 0.14 ms; first spike, 1.07 ± 0.14 ms) cell groups.

The minimum peak response latency of unit discharges was determined in 18 TRN-MGV and 18 TRN-MGD cells. In the other cells, the peak response latency could not be determined because there was no cell activity within 100 ms (two TRN-MGV cells) or a peak of cell activity was not clear in primary response (six TRN-MGV and four TRN-MGD cells). The minimum peak response latency was significantly shorter ($t_{34} = 4.55$, $P < 0.0001$) for the TRN-MGV cell group (18.94 ± 6.14 ms) than for the TRN-MGD cell group (37.27 ± 15.96 ms). In spontaneous activity, oscillation of 3–4 Hz was observed in one case in each of the TRN-MGV and TRN-MGD cell groups. There was no noticeable difference in the pattern of spontaneous activity between the TRN-MGV and TRN-MGD cell groups as represented in the auto-correlation functions of cases 011613-5 and 031512-8 (Figs 1B and 2B).

Effects of sensory and recurrent activations on burst spiking

It is presumed that cortical and thalamic inputs to TRN cells are repeatedly recruited following sensory stimulation (sensory activation) in the loop connections between cortical areas and thalamic nuclei (Pinault, 2003). The recruited inputs are considered to drive TRN cell activity after the end of sensory stimulation (recurrent activation) in conjunction with the intrinsically generated oscillatory activation of TRN cells (Steriade *et al.*, 1987). To compare the effects of sensory and recurrent activations on burst spiking (Fig. 6), the features (the number of spikes composing a burst and averaged

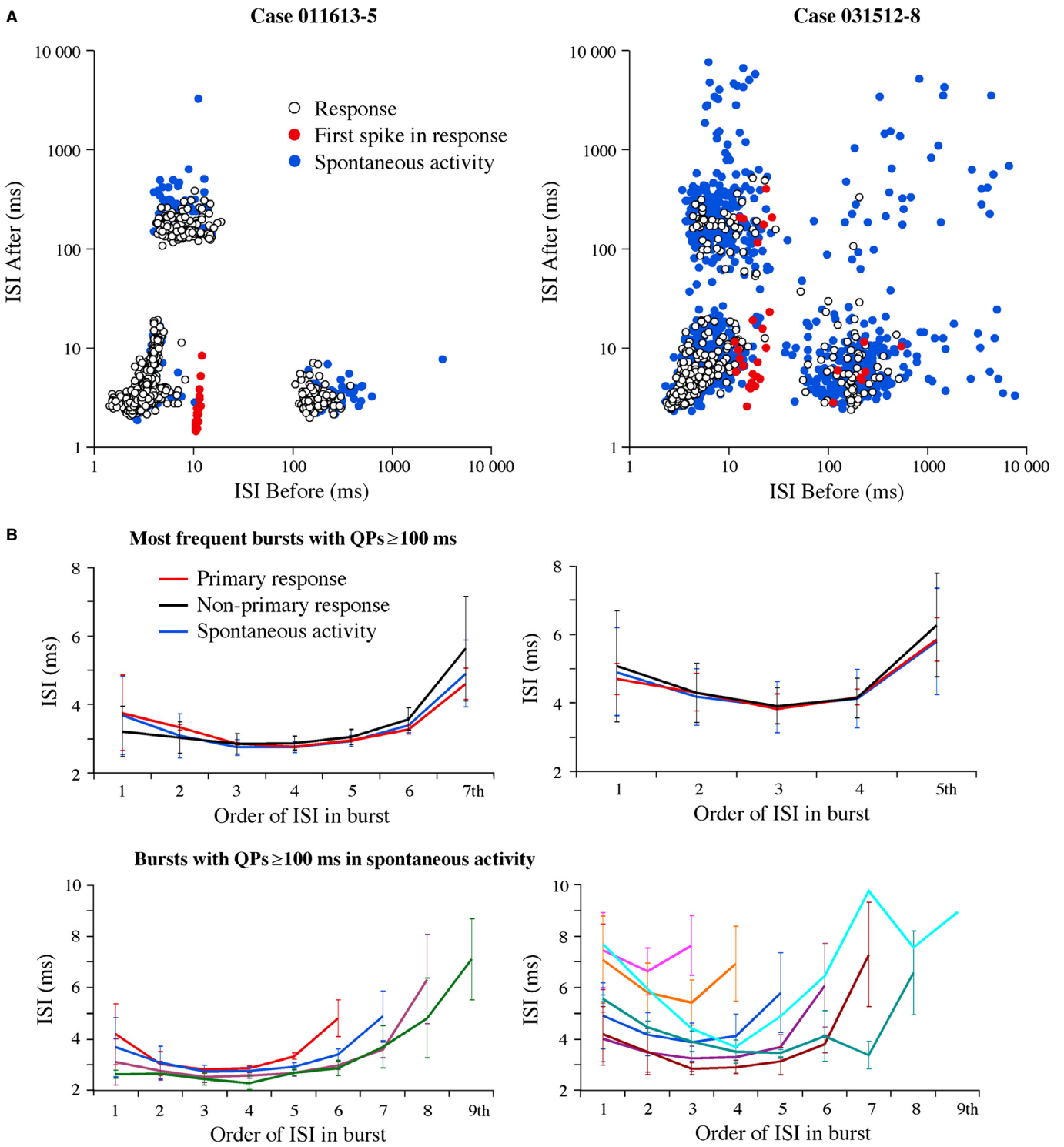

FIG. 4. ISI plots and intra-burst ISI profiles. (A) ISIs before and after a spike were measured in recordings of auditory response (white circles) and spontaneous activity (blue circles). ISI after the first spike in auditory response was also plotted (red circles) together with its response latency as ISI before the spike. (B) Upper graphs indicate the relationship between the order and length (mean ± SD, ms) of ISI in the most frequently observed bursts that were composed of eight spikes in case 011613-5 (left) and six spikes in case 031512-8 (right). Similar intra-burst ISI profiles (an initial progressive decrease followed by a progressive increase of length) were observed in bursts preceded by QPs ≥ 100 ms in primary (red lines), non-primary auditory responses (black lines) and spontaneous activity (blue lines). Lower graphs indicate intra-burst ISI profiles of all bursts preceded by QPs ≥ 100 ms in spontaneous activity.

intra-burst ISI) of burst spiking in all bursts in primary response, which were assumed to represent burst spiking in cell activity directly driven by auditory inputs ascending from thalamic nuclei (Kimura, 2014), were compared (paired *t*-test) with those of burst spiking in non-primary response (recurrent activation). Two cases in the TRN-MGV cell group were excluded from this data analysis because of the absence of discharge events in primary response. There were no significant differences (number of spikes, $t_{23} = 0.46$,

TABLE 1. Comparisons in the features of auditory response between TRN-MGV and TRN-MGD cell groups; values are mean ± SD

	TRN-MGV (n = 26 cells)	TRN-MGD (n = 22 cells)
All events (primary and non-primary responses)		
No. of events (/s)	3.17 ± 2.20	2.73 ± 2.67
No. of spikes (/s)*	16.00 ± 9.10	7.94 ± 3.86
% of burst spiking*	78.7 ± 13.5	59.4 ± 27.3
No. of spikes in burst*	6.73 ± 1.61	4.87 ± 1.33
Averaged ISI in burst (ms)*	4.03 ± 0.90	5.34 ± 1.13
First ISI in burst (ms)*	4.48 ± 1.12	5.91 ± 1.40
Events with QPs ≥ 100 ms (non-primary response)		
No. of events (/s)	1.89 ± 1.10	1.43 ± 0.67
No. of spikes (/s)*	11.71 ± 7.16	5.43 ± 3.40
% of burst spiking*	92.6 ± 9.1	71.6 ± 27.7
No. of spikes in burst*	6.81 ± 1.52	5.19 ± 1.45
Averaged ISI in burst (ms)*	4.01 ± 0.87	5.25 ± 1.04
First ISI in burst (ms)*	4.45 ± 1.11	5.96 ± 1.35

QP, quiescent period; *$P < 0.05$, corrected for multiple comparisons.

$P = 1$; averaged ISI, $t_{23} = 0.17$, $P = 1$) in the features of burst spiking in the TRN-MGV cell group (Figs 6A and B), while the numbers of spikes composing a burst were smaller ($t_{21} = 2.45$, $P = 0.0461$) and averaged intra-burst ISIs tended to be longer ($t_{21} = 2.20$, $P = 0.0786$) for burst spiking in primary response (sensory activation) in the TRN-MGD cell group (Figs 6C and D). Furthermore, the features of burst spiking in all bursts in non-primary response were compared with those of burst spiking in spontaneous activity so as to determine possible sustained effects of auditory inputs on burst spiking in recurrent activation. In the TRN-MGV cell group ($n = 12$), there were significant differences when data obtained from a peculiar case (white circles with asterisks in Figs 6E and F) were excluded from data analysis: the numbers of spikes composing a burst and averaged intra-burst ISIs were smaller ($t_{10} = 3.47$, $P = 0.0121$) and longer ($t_{10} = 3.34$, $P = 0.0149$), respectively, for burst spiking in recurrent activation. In the TRN-MGD cell group ($n = 13$), there were no significant differences (number of spikes, $t_{12} = 2.08$, $P = 0.1195$; averaged ISI, $t_{12} = 0.80$, $P = 0.8836$) (Figs 6G and H). The results were summarized as follows: sound stimulation sustainably affected the properties of burst spiking of TRN-MGV cells in their non-primary responses (recurrent activation), whereas it transiently affected those of TRN-MGD cells in their primary responses (direct sensory activation).

Locations of cell bodies and topographies of axonal projections

Labeled cells were located mainly in the ventral sector of the TRN from 3.3 to 4.5 mm posterior to bregma (Fig. 7A). The distributions of TRN-MGV ($n = 25$) and TRN-MGD cells ($n = 22$) were biased toward the rostroventral and caudodorsal sides, respectively: the locations of TRN-MGV cells significantly differed from those of TRN-MGD cells along the rostrocaudal ($t_{45} = 2.86$, $P = 0.0123$) and dorsoventral neural axes ($t_{45} = 2.45$, $P = 0.0361$). Many TRN-MGV cells were located in the lateral tier (cells in the medial tier, six; lateral tier, 14; middle, five), while TRN-MGD cells were primarily located in the medial tier (cells in the medial tier, 16; lateral tier, four; middle two).

The locations of terminal fields in the three-dimensional extent of the MGV and the rostrocaudal extent of the MGD were examined to determine the topographies of axonal projections. Axonal projections were topographic in a similar manner along the rostrocaudal neural axis in the TRN-MGV ($r_{23} = 0.56$, $P = 0.0180$, Pearson's correlation coefficient test) and TRN-MGD cell groups ($r_{20} = 0.58$, $P = 0.0072$): the more rostrally located cells sent axonal projections to the more rostral portions of the MGV and MGD (Fig. 7B). As has been reported in a previous study (Kimura *et al.*, 2007), the more rostrally located TRN-MGV cells sent axonal projections to the more ventral portions of the MGV ($r_{23} = 0.50$, $P = 0.0618$) and the more ventrally located TRN-MGV cells sent axonal projections to the more ventral ($r_{23} = 0.51$, $P = 0.0468$) and medial portions ($r_{23} = 0.70$, $P = 0.0006$) of the MGV (data not shown). The dorsoventral locations of cell bodies did not correlate with the rostrocaudal locations of terminal fields in both the TRN-MGV ($r_{23} = 0.03$, $P = 1$) and the TRN-MGD cell groups ($r_{20} = 0.003$, $P = 1$).

Correlations between the features of burst spiking and the locations of cell bodies and terminal fields

In light of the correlations between the features of burst spiking and the locations of cell bodies and terminal fields in TRN visual cells (Kimura *et al.*, 2012b), we examined relationships between the features (number of spikes composing a burst, and averaged and first intra-burst ISIs) of burst spiking and the locations of cell bodies and terminal fields in TRN auditory cells (Fig. 8). The numbers of spikes composing a burst correlated with the rostrocaudal locations of cell bodies (Figs 8A and E) and terminal fields in the TRN-MGD cell group (Figs 8C and F): the numbers of spikes composing a burst in all bursts increased as cell bodies or terminal fields were more rostrally located in both the whole auditory response (cell body, $r_{20} = 0.72$, $P = 0.0006$; terminal field, $r_{20} = 0.74$, $P = 0.0003$; Pearson's correlation coefficient test) and spontaneous activity (cell body, $r_{11} = 0.79$, $P = 0.0036$; terminal field, $r_{11} = 0.70$, $P = 0.0201$). Similar results were obtained from data analysis of bursts with preceding QPs ≥ 100 ms in non-primary response (cell body, $r_{20} = 0.71$, $P = 0.0006$; terminal field, $r_{20} = 0.73$, $P = 0.0003$) and spontaneous activity (cell body, $r_{11} = 0.79$, $P = 0.0036$; terminal field, $r_{11} = 0.75$, $P = 0.0066$) (data not shown). In the TRN-MGV cell group, first intra-burst ISIs of all bursts in the whole auditory response tended to correlate ($r_{23} = -0.42$, $P = 0.0714$) with the rostrocaudal locations of cell bodies (Fig. 8B), and first (data not shown) and averaged intra-burst ISIs (Fig. 8D) of all bursts in the whole auditory response correlated ($r_{24} = -0.56$, $P = 0.0243$; $r_{24} = -0.65$, $P = 0.0018$) with the rostrocaudal locations of terminal fields: intra-burst ISIs became shorter as cell bodies or terminal fields were more rostrally located. Similar correlations were found in bursts with preceding QPs ≥ 100 ms in non-primary auditory response (first ISI – cell body, $r_{23} = -0.52$, $P = 0.0444$; first ISI – terminal field, $r_{24} = -0.62$, $P = 0.0054$; averaged ISI – terminal field, $r_{24} = -0.54$, $P = 0.0306$) (data not shown). Averaged ISIs of TRN-MGD cells also tended to be shorter ($r_{20} = -0.48$, $P = 0.0669$) as their terminal fields were more rostrally located in their bursts with preceding QPs ≥ 100 ms in non-primary auditory response (data not shown). There were no correlations between intra-burst ISIs and the locations of cell bodies and terminal fields in spontaneous activity. In summary, the ISIs and numbers of spikes in burst spiking correlated with the locations of cell bodies and terminal fields in the TRN-MGV and TRN-MGD cell groups, respectively: the more rostrally located TRN-MGV and TRN-MGD cells projecting to the more rostral portions of the MG showed the more intense burst spiking in terms of the density (TRN-MGV cells) and number of

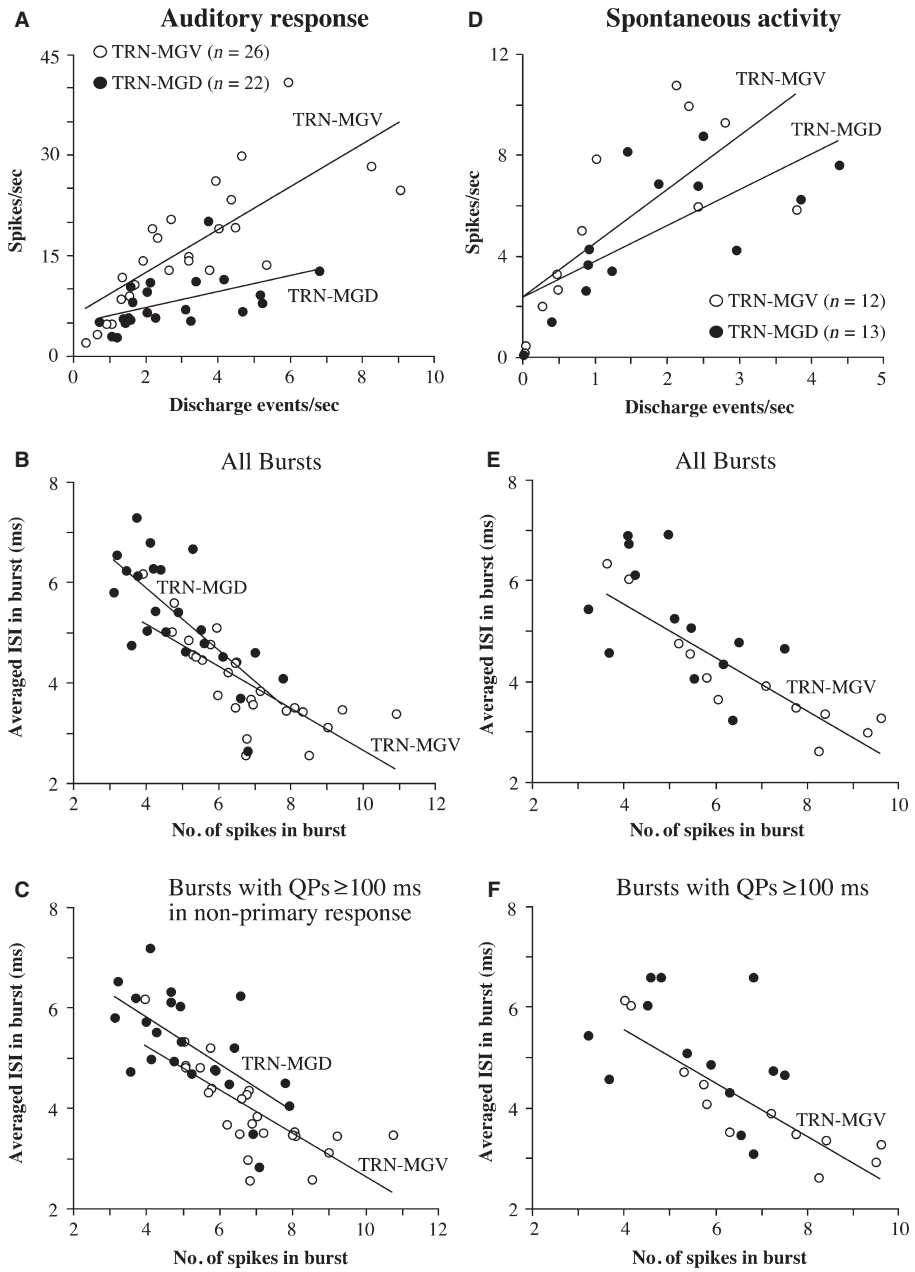

FIG. 5. Features of auditory responses (A–C) and spontaneous activities (D–F) in the TRN-MGV and TRN-MGD cell groups. (A) In the whole auditory response, TRN-MGV cells (white circles) showed higher spike rates per noise burst stimulus (ordinate) than TRN-MGD cells (black circles), although there was no difference in the incidence of discharge events (abscissa). The numbers of discharge events and those of spikes were correlated in both the TRN-MGV and the TRN-MGD cell groups (continuous regression lines). The slope of the regression line in the TRN-MGV cell group differed from that in the TRN-MGD cell group. (B,C) TRN-MGV cells showed bursts with larger numbers of spikes and shorter averaged ISIs in all bursts in the whole auditory response and bursts with preceding QPs ≥ 100 ms in non-primary auditory response. The numbers of spikes and averaged ISIs in bursts were correlated in both the TRN-MGV and the TRN-MGD cell groups (continuous regression lines). The slopes of the regression lines in the TRN-MGV cell group did not differ from those in the TRN-MGD cell group. (D) In spontaneous activities, there were no differences in the numbers of discharge events and spikes between the TRN-MGV and TRN-MGD cell groups. The numbers of discharge events and those of spikes were correlated in both the TRN-MGV and TRN-MGD groups (continuous regression lines). There was no difference in the slope of the regression line between the TRN-MGV and TRN-MGD cell groups. (E) Averaged ISIs in the TRN-MGV cell group tended to be shorter than those in the TRN-MGD cell group in all bursts; however, this was not statistically significant. There were no differences in the number of spikes composing a burst (abscissa in E and F) and averaged ISI in bursts with preceding QPs ≥ 100 ms (ordinate in F) between the TRN-MGV and TRN-MGD cell groups. The numbers of spikes and averaged ISIs were correlated in the TRN-MGV cell group (continuous regression lines) but not in the TRN-MGD cell group (E and F).

spikes (TRN-MGD cells) composing a burst. In the TRN-MGV cell group the correlations were observed only in auditory response, while in the TRN-MGD cell group the correlations were observed in both auditory response and spontaneous activity.

Correlations between the features of burst spiking and the locations of cell bodies across sensory modalities

Auditory and visual cells are distributed in the ventral and dorsal portions of a largely similar rostrocaudal range of the TRN (Kimura

TABLE 2. Comparisons in the features of spontaneous activity between TRN-MGV and TRN-MGD cell groups; values are mean ± SD

	TRN-MGV (n = 12 cells)	TRN-MG (n = 13 cells)
All events		
No. of events (/s)	1.38 ± 1.25	1.83 ± 1.33
No. of spikes (/s)	5.27 ± 3.65	4.93 ± 2.69
% of burst spiking	74.3 ± 22.8	58.3 ± 28.8
No. of spikes in burst	6.72 ± 1.98	5.15 ± 1.26
Averaged ISI in burst (ms)	4.08 ± 1.15	5.23 ± 1.15
First ISI in burst (ms)	4.51 ± 1.37	5.94 ± 1.51
Events with QPs ≥ 100 ms		
No. of events (/s)	0.88 ± 0.69	0.91 ± 0.53
No. of spikes (/s)	4.38 ± 2.91	3.34 ± 2.08
% of burst spiking	90.0 ± 19.9	70.2 ± 31.8
No. of spikes in burst	6.84 ± 1.91	5.64 ± 1.39
Averaged ISI in burst (ms)	4.04 ± 1.12	5.07 ± 1.14
First ISI in burst (ms)	4.48 ± 1.32	5.98 ± 1.75

QP, quiescent period.

et al., 2012b; Kimura, 2014). The present and previous results (Kimura *et al.*, 2012b) indicated that there are correlations between the features of burst spiking and the rostrocaudal locations of cell bodies in both auditory and visual cells. It was suggested therefore that there could be a common structural basis that correlates the features (number of spikes composing a burst and averaged intra-burst ISI) of burst spiking with the rostrocaudal locations of cell bodies across sensory modalities. The relationships between the features of burst spiking in spontaneous activity and the rostrocaudal locations of cell bodies were examined in a database of auditory (n = 24) and visual cells (n = 15) that included the two types of cells projecting to first- and higher-order thalamic nuclei. Data of visual cells (six and nine visual cells projecting to the DLG and LP) were obtained from a previous study (Kimura *et al.*, 2012b). The numbers of spikes composing a burst correlated with the rostrocaudal locations of cell bodies in both auditory cells (all bursts, $r_{22} = 0.53$, $P = 0.0414$; bursts with preceding QPs ≥ 100 ms, $r_{22} = 0.56$, $P = 0.0234$; Pearson's correlation coefficient test) and visual cells ($r_{13} = 0.75$, $P = 0.0048$; $r_{13} = 0.73$, $P = 0.0084$): cells located in the more rostral side exhibited burst spiking with the larger numbers of spikes (Fig. 9A). The slope of the regression line in auditory cells did not differ from that in visual cells (all bursts, $t_{35} = 0.10$, $P = 0.9235$; bursts with preceding QPs ≥ 100 ms, $t_{35} = 0.04$, $P = 0.9652$), and strong correlations (all bursts, $r_{37} = 0.66$, $P = 0.0006$; bursts with preceding QPs ≥ 100 ms, $r_{37} = 0.66$, $P = 0.0006$) were calculated when the data of auditory and visual cells were combined. Averaged intra-burst ISIs tended to be shorter in the more rostrally located visual cells (all bursts, $r_{13} = -0.64$, $P = 0.0546$; bursts with preceding QPs ≥ 100 ms, $r_{13} = -0.64$, $P = 0.0534$) (Fig. 9B). Although there was no correlation in auditory cells (all bursts, $r_{22} = -0.43$, $P = 0.2202$; bursts with preceding QPs ≥ 100 ms, $r_{22} = -0.44$, $P = 0.1914$), strong correlations (all bursts, $r_{37} = -0.46$, $P = 0.0162$; bursts with preceding QPs ≥ 100 ms, $r_{37} = -0.48$, $P = 0.0102$) were calculated when the data of auditory and visual cells were combined.

Burst spiking with long intra-burst ISIs and short preceding QPs

In a subset of cases (five TRN-MGV and 15 TRN-MGD cells) there were trains of spikes with ISIs exceeding 10 ms, some of which were preceded by QPs shorter than 100 ms (right graph in Fig. 4A). It was suggested therefore that some bursts could have intra-burst ISIs and preceding QPs out of the ranges applied to detect burst spiking in the above data analysis (Domich *et al.*, 1986; Shosaku *et al.*, 1989; Sumitomo *et al.*, 1989). In view of the finding that in most cases possible long intra-burst ISIs did not exceed 20 ms and possible short preceding QPs were over 50 ms (right graph in Fig. 4A), data were analysed again, detecting trains of spikes with ISIs < 20 ms as bursts, which, when preceded by QPs ≥ 50 ms, were then considered to represent LTS bursts. As a result, putative LTS bursts with preceding QPs ≥ 50 ms were found to have the pattern of intra-burst ISIs (an initial progressive decrease followed by a progressive increase of ISI) peculiar to LTS burst in both auditory response and spontaneous activity (Fig. 10A). The same three cells showed an exceptional pattern of intra-burst ISIs (first ISIs shorter than second ISIs).

Results (data not shown) similar to those in the above data analysis were obtained with regard to the numbers of discharge events and spikes (data analyses comparable to those indicated in Figs 5A and D). There were no differences in the numbers of all discharge events and events with preceding QPs ≥ 50 ms between the TRN-MGV and TRN-MGD cell groups in both auditory response and spontaneous activity (Table 3). The number of spikes in discharge events with preceding QPs ≥ 50 ms in the TRN-MGV cell group differed ($t_{46} = 3.47$, $P = 0.0023$) from that in the TRN-MGD cell group in auditory response, but not in spontaneous activity. The slope of the regression line in the relationship between the numbers of discharge events and spikes in the TRN-MGV cell group also differed ($t_{44} = 2.58$, $P = 0.0134$) from that in the TRN-MGD cell group in all discharge events in the whole auditory response but not in discharge events with preceding QPs ≥ 50 ms in non-primary response. Like the results in the above data analysis (Table 1, Figs 5B and C) the features of burst spiking in the TRN-MGV cell group were distinct from those in the TRN-MGD cell group in auditory response (Table 3): all bursts and bursts with preceding QPs ≥ 50 ms in the TRN-MGV cell group appeared at higher incidences (all bursts, $t_{46} = 3.47$, $P = 0.0046$; bursts with preceding QPs ≥ 50 ms, $t_{46} = 3.28$, $P = 0.0079$) and were composed of larger numbers of spikes (all bursts, $t_{46} = 4.33$, $P = 0.0003$; bursts with preceding QPs ≥ 50 ms, $t_{46} = 3.95$, $P = 0.0011$) with shorter averaged ISIs (all bursts, $t_{46} = 4.30$, $P = 0.0004$; bursts with preceding QPs ≥ 50 ms, $t_{46} = 4.24$, $P = 0.0004$) and first ISIs (all bursts, $t_{46} = 3.98$, $P = 0.0010$; bursts with preceding QPs ≥ 50 ms, $t_{46} = 4.23$, $P = 0.0004$) as compared with all bursts and bursts with preceding QPs ≥ 50 ms in the TRN-MGD cell group (left graph in Fig. 10B). The results with regard to the correlation (all bursts in primary and non-primary responses; TRN-MGV cells, $r_{24} = -0.72$, $P = 0.0004$; TRN-MGD cells, $r_{20} = -0.60$, $P = 0.0100$; bursts with preceding QPs ≥ 50 ms in non-primary response; TRN-MGV cells, $r_{24} = -0.73$, $P = 0.0004$; TRN-MGD cells, $r_{20} = -0.59$, $P = 0.0136$) and the slope of the regression line (all bursts in primary and non-primary responses, $t_{44} = 1.34$, $P = 0.1878$; bursts with preceding QPs ≥ 50 ms in non-primary response, $t_{44} = 0.96$, $P = 0.3424$) in the relationship between the number of spikes composing a burst and averaged ISI (left graph in Fig. 10B) was similar to those in the above data analysis (Fig. 5B and C). In spontaneous activity (Table 3), there was no difference in the incidence of burst spiking, the number of spikes composing a burst and averaged intra-burst ISI between the TRN-MGV and TRN-MGD cell groups (right graph in Fig. 10B), while first intra-burst ISIs in the TRN-MGV cell group tended to differ (all bursts, $t_{23} = 2.44$, $P = 0.0911$; bursts with preceding QPs ≥ 50 ms, $t_{23} = 2.41$, $P = 0.0975$) from those in TRN-MGD cell group.

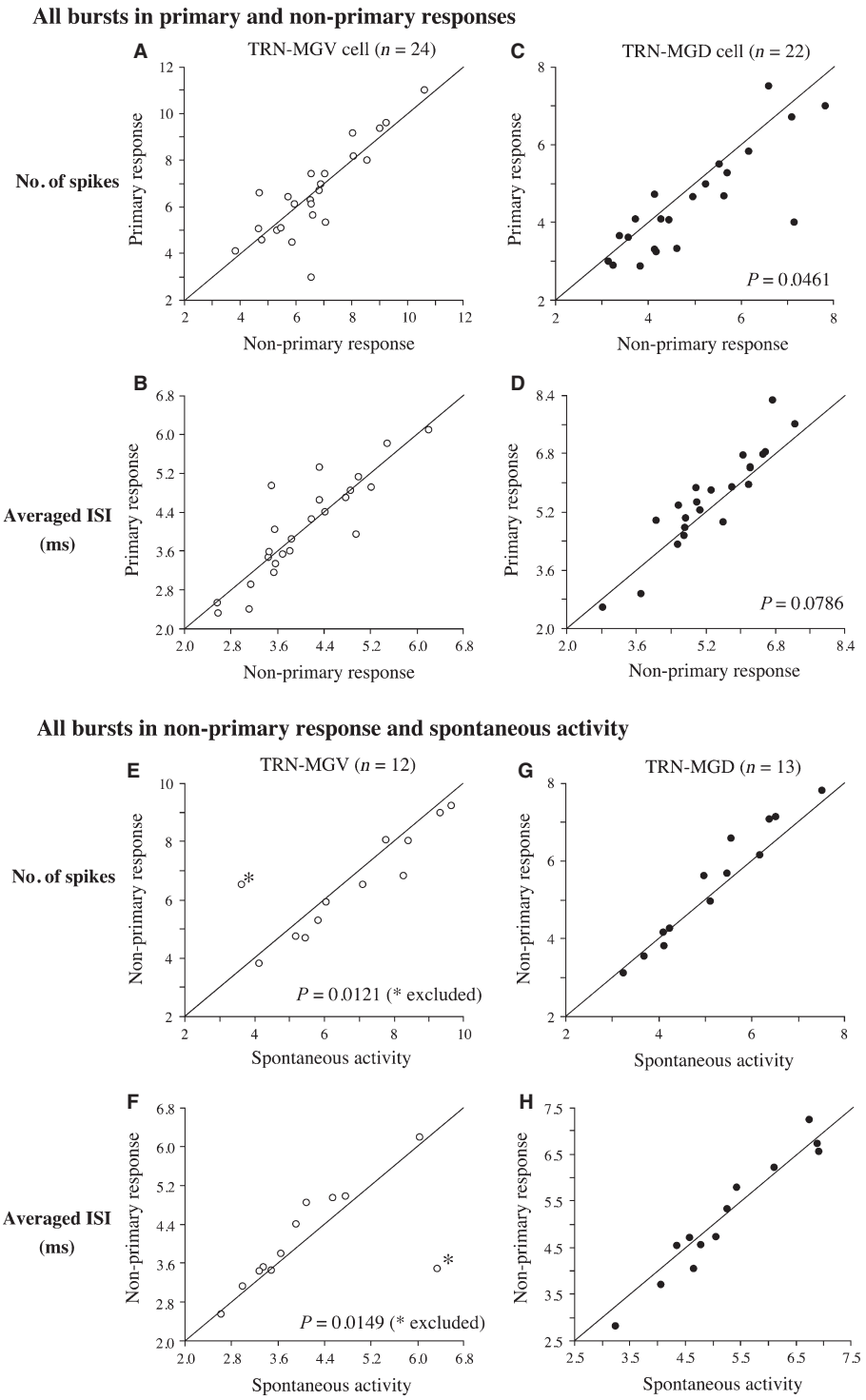

FIG. 6. Features of burst spiking in sensory and recurrent activations. There were no differences in the features of burst spiking in all bursts between primary and non-primary responses (sensory and recurrent activations) in the TRN-MGV cell group (A and B), while in the TRN-MGD cell group the numbers of spikes composing a burst and averaged intra-burst ISIs in primary response were smaller and longer than those in non-primary response (C and D). In the TRN-MGV cell group the numbers of spikes composing a burst and averaged intra-burst ISIs in non-primary response were smaller and longer than those in spontaneous activity except in a peculiar case (asterisks) (E and F), while there were no differences between non-primary response and spontaneous activity in the TRN-MGD cell group (G and H).

In comparisons (paired *t*-test) between the features of burst spiking in all discharge events of primary response and those of burst spiking in all discharge events of non-primary response (data analyses comparable to those indicated in Figs 6A–D), a similar difference (smaller numbers of spikes composing a burst in primary response), although not statistically significant ($t_{21} = 2.24$, $P = 0.0720$), was observed only in the number of spikes composing a burst in the TRN-MGD cell group. In comparisons between the

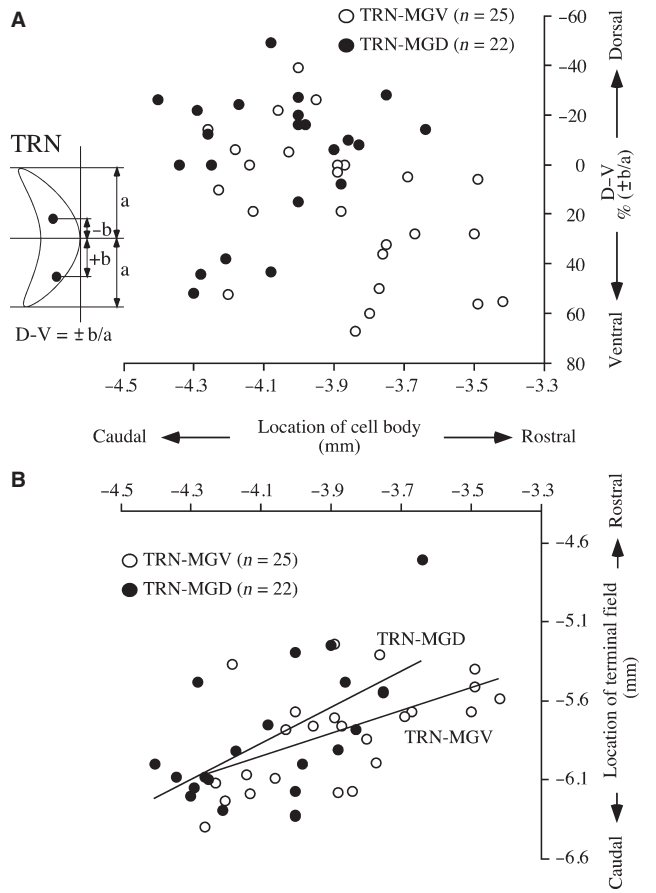

FIG. 7. Locations of cell bodies and terminal fields. (A) The locations of TRN-MGV and TRN-MGD cells (white and black circles) were biased toward the rostroventral and caudodorsal portions of the TRN, respectively. (B) Both TRN-MGV and TRN-MGD cells sent topographic projections to the MGV and MGD along the rostrocaudal neural axis (continuous regression lines).

features of burst spiking in all discharge events with preceding periods ≥ 50 ms in non-primary auditory response and those in spontaneous activity (data analyses comparable to those indicated in Figs 6E–H), similar significant differences (smaller numbers of spikes composing a burst and longer averaged ISIs in non-primary auditory response) were observed in the number of spikes composing a burst ($t_{10} = -3.41$, $P = 0.0132$) and averaged ISI ($t_{10} = 3.56$, $P = 0.0103$) of the TRN-MGV cell group when data from a peculiar case (the same case noted in the above data analysis) were excluded from data analysis.

With regard to the relationships between the features of burst spiking and the locations of cell bodies (data analyses comparable to those indicated in Figs 8A, B and E), the numbers of spikes composing a burst correlated (all bursts in auditory response, $r_{20} = 0.72$, $P = 0.0006$; bursts with preceding QPs ≥ 50 ms in non-primary auditory response, $r_{20} = 0.70$, $P = 0.0006$; all bursts in spontaneous activity, $r_{11} = 0.78$, $P = 0.0054$; bursts with preceding QPs ≥ 50 ms, $r_{11} = 0.79$, $P = 0.0042$) with the rostrocaudal locations of cell bodies in the TRN-MGD cell group, as with the results in the above data analysis, but no correlation was observed between first ISIs and the rostrocaudal locations of cell bodies in the TRN-MGV cell group, unlike the results in the above data analysis. With regard to the relationships between the features of burst spiking and the locations of terminal fields (data analyses comparable to those indicated in Figs 8C, D and F), the numbers of spikes composing a burst correlated (all bursts in auditory response, $r_{20} = 0.70$, $P = 0.0006$; bursts with preceding QPs ≥ 50 ms in non-primary auditory response, $r_{20} = 0.70$, $P = 0.0006$; all bursts in spontaneous activity, $r_{11} = 0.73$, $P = 0.0111$; bursts with preceding QPs ≥ 50 ms, $r_{11} = 0.73$, $P = 0.0105$) with the rostrocaudal locations of terminal fields in the TRN-MGD cell group, as with the results in the above data analysis, but correlations (all bursts in auditory response, $r_{24} = -0.58$, $P = 0.0126$; bursts with preceding quiescent in non-primary auditory response, $r_{24} = -0.53$, $P = 0.0423$) were observed only between first ISIs and the rostrocaudal locations of terminal fields in the TRN-MGV cell group, unlike the results in the above data analysis.

In conclusion, similar results were obtained from the data analysis of burst spiking with long intra-burst ISIs (< 20 ms) and short preceding QPs (≥ 50 ms): TRN-MGV cells had higher propensities for burst spiking with larger numbers of spikes and shorter ISIs as compared with TRN-MGD cells in auditory response, and similar distinctions, although not statistically significant, were observed in spontaneous activity (Table 3 and Fig. 10). The results were also similar with regard to the alterations of burst spiking in primary and non-primary responses and the associations between the variations of burst spiking and the topographies of cell body and terminal field locations.

Discussion

The results are summarized as follows. In auditory response, TRN-MGV cells had higher propensities for burst spiking and exhibited bursts of larger numbers of spikes with shorter ISIs as compared with TRN-MGD cells. Similar distinctions, although not statistically different, were observed in spontaneous activity. The features of burst spiking varied in association with the topographies of cell body and terminal field locations. Sound stimulation altered the features of burst spiking in non-primary responses of TRN-MGV cells but not those of TRN-MGD cells. Similar findings have been obtained from TRN visual cells projecting to the DLG and LP (Kimura *et al.*, 2012b). Therefore, it is postulated that TRN cells projecting to first- and higher-order thalamic nuclei have high and low levels of burst spiking across sensory modalities, which contrast with low and high levels of burst spiking in first- (the MGV and DLG) and higher-order (the MGD and LP) thalamic nuclei (He & Hu, 2002; Ramcharan *et al.*, 2005; Wei *et al.*, 2011). Furthermore, the features of burst spiking are associated with afferent and efferent connectivities of the TRN in a similar manner across sensory modalities.

Distinctions in the features of burst spiking between TRN cells projecting to first- and higher-order thalamic nuclei

In both auditory and visual modalities, high and low levels of burst spiking are recognized in the two groups of TRN cells projecting to first- and higher-order thalamic nuclei. A question arises as to whether these distinct levels of burst spiking reflect differences in extrinsically conditioned states of synaptic activation or differences in intrinsically determined cell membrane properties. The present results seem to support the former possibility. The slopes of regression lines of the number of spikes and ISI in the TRN-MGV cell group did not differ from those in the TRN-MGD cell group (Figs 5B, C, and 10B), suggesting that the two cell groups have common cell membrane properties for burst spiking, which could generate various levels of burst spiking depending on

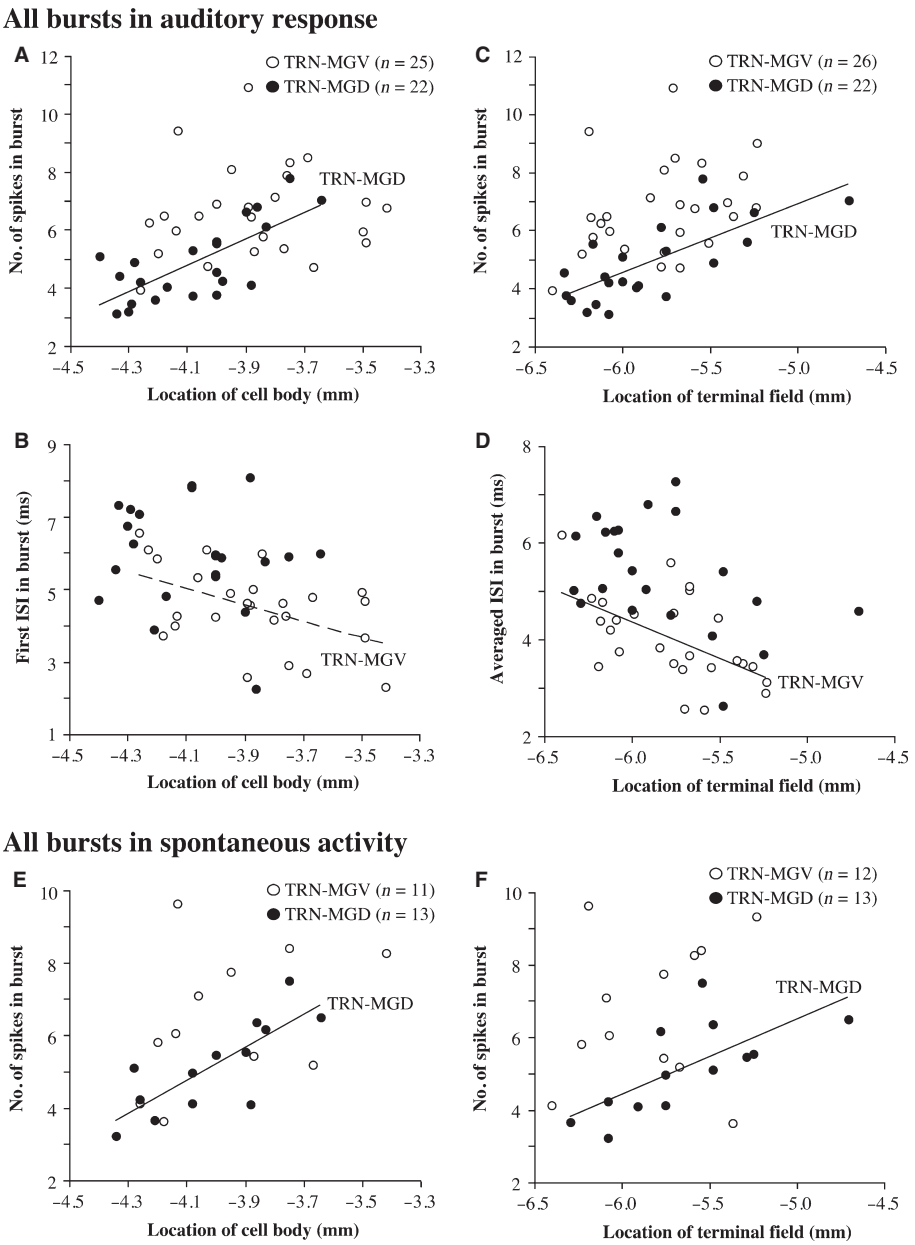

FIG. 8. Relationships between the features of burst spiking and the locations of cell bodies and terminal fields. The numbers of spikes composing a burst in all bursts correlated (continuous regression lines) with the rostrocaudal locations of TRN-MGD cells (black circles) in the whole auditory response (A) and spontaneous activity (E). There was a weak correlation (dotted regression line) between first intra-burst ISIs in all bursts and the rostrocaudal locations of TRN-MGV cells (white circles) in the whole auditory response (B). The numbers of spikes composing a burst in all bursts correlated (continuous regression lines) with the rostrocaudal locations of terminal fields in the TRN-MGD cell group (black circles) in the whole auditory response (C) and spontaneous activity (F). There was a correlation (continuous regression line) between averaged intra-burst ISIs in all bursts and the rostrocaudal locations of terminal fields in the TRN-MGV cell group (white circles) in the whole auditory response (D).

the states of synaptic activation. Accordingly, the distinctions in burst spiking between the two groups were apparent in auditory response, i.e. at the moment of intense synaptic activation, but not in spontaneous activity. Considering cell body locations and response latencies, TRN-MGV and TRN-MGD cells are highly likely to receive auditory inputs from the MGV and MGD (Bordi & LeDoux, 1994; Kimura *et al.*, 2003, 2012a). The distinctions in burst spiking could be then ascribed to differences in the impacts of auditory inputs ascending through the MGV and MGD. Note, however, that the distinctions in burst spiking were apparent in non-primary as well as primary response and that similar distinctions, although not statistically significant, were observed in spontaneous activity. These findings suggest that TRN-MGV and TRN-MGD cells were preconditioned to show distinct patterns of spiking in response to intense synaptic activation by auditory inputs. The distinctions in burst spiking in visual cells, which appear more remarkable than those in auditory cells, are apparent in spontaneous activity as well (Kimura *et al.*, 2012b). This supports the possibility.

The distinctions in burst spiking were observed in putative LTS bursts. As a hyperpolarized state is a prerequisite for a cell to generate LTS burst (Llinás & Steriade, 2006), it is postulated that

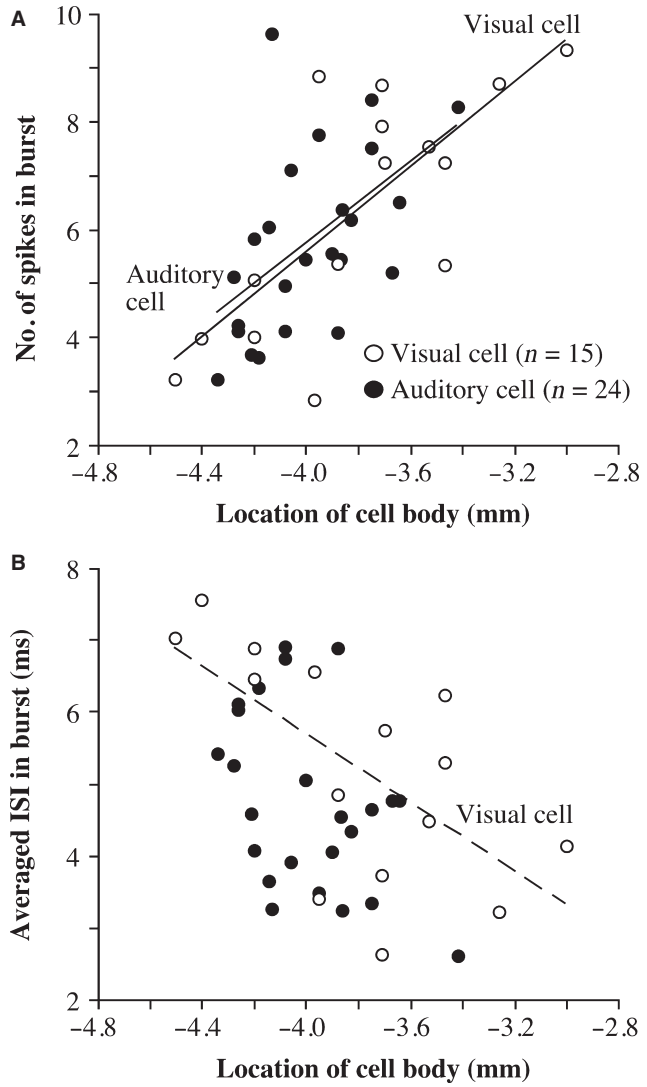

FIG. 9. Features of burst spiking associated with cell body locations across auditory and visual modalities. (A) In spontaneous activity, the numbers of spikes composing a burst in all bursts correlated (continuous regression lines) with the rostrocaudal locations of cell bodies in both auditory and visual cell groups (black and white circles). A higher correlation was calculated when the data of auditory and visual cells were combined. (B) There was a weak correlation (dotted regression line) between averaged intra-burst ISIs in all bursts and the rostrocaudal locations of visual cells (white circles). Despite the absence of a correlation in the auditory cell group (black circles), a statistically significant correlation was calculated when the data of auditory and visual cells were combined.

TRN-MGV cells are embedded in relatively hyperpolarized states to show more frequently burst spiking (Sumitomo *et al.*, 1989). On the other hand, TRN-MGD cells could be embedded in relatively depolarized states that hamper the generation of burst spiking. The finding that the incidences of burst spiking in TRN-MGV and TRN-MGD cell groups were high and low in the discharge events preceded by QPs (another prerequisite for the generation of LTS burst) also suggests that the states of TRN-MGV and TRN-MGD cells were biased toward hyperpolarization and depolarization. As a possibility, TRN-MGV and TRN-MGD cells may be conditioned to such different states under the barrages of excitatory inputs from the MGV and MGD, which, with low and high levels of burst spiking (He & Hu, 2002; Ramcharan *et al.*, 2005), could depolarize TRN cells in different manners. An important finding is that sound stimulation altered burst spiking in non-primary responses of TRN-MGV cells but not in those of TRN-MGD cells. Non-primary response is considered to be driven by cortical and thalamic inputs repeatedly recruited following sound stimulation in the thalamocortical loop (Steriade, 2006; Huguenard & McCormick, 2007; Jones, 2009) that interact with intrinsically generated oscillatory activation of TRN cells (Steriade *et al.*, 1987; Zaman *et al.*, 2011). Effects of light stimulation on burst spiking in non-primary response are also observed in TRN visual cells projecting to the DLG but not in those projecting to the LP (Kimura *et al.*, 2012b). As such, across sensory modalities, thalamocortical loop circuitries that include the two types of TRN cells differ from each other in a similar manner with regard to the temporal sensitivity to sensory activation. It could be further assumed that the distinctions in burst spiking between the two types of TRN cells represent the states of cell activity differentially conditioned by the thalamocortical loop circuitries, probably in conjunction with mutual cell connectivity inside the TRN (Landisman *et al.*, 2002; Sohal & Huguenard, 2003; Sun *et al.*, 2012).

It is possible that the distinctions in burst spiking derive from heterogeneous intrinsic membrane properties. In slice preparations cells in the putative auditory and visual domains of the TRN are categorized into Typical-, Atypical- and Non-burst types that have heterogeneous membrane properties (Lee *et al.*, 2007). In line with the predominance of Typical-burst type in the putative auditory domain, TRN cells examined in the present study are all likely to correspond to Typical-burst type characterized by an initial decrease of intra-burst ISI, except three cells which are considered to be Atypical type characterized by an initial increase of intra-burst ISI. Therefore, it seems plausible to postulate that TRN cells examined in the present study are virtually homogenous in terms of intrinsic membrane properties, as also suggested by their identical spike widths (Lee *et al.*, 2007).

As pentobarbital alters cellular and/or circuitry propensity for oscillation (Cotillon-Williams & Edeline, 2003) and burst spiking (Massaux *et al.*, 2004), it is unclear whether the distinctions in burst spiking between the TRN-MGV and TRN-MGD cell groups observed in the present results could be replicated as the aspects of physiological function in non-anesthetized animals. It has been shown, however, that pentobarbital does not affect the properties (the number of spikes and ISI in a burst) of burst spiking in thalamic nuclei (Massaux & Edeline, 2003; Massaux *et al.*, 2004). The present and previous results (Kimura *et al.*, 2012b) indicate similar distinctions in burst spiking between TRN cells projecting to first- and higher-order thalamic nuclei across auditory and visual modalities, although there is a clear difference in the density of GABAergic interneurons in auditory and visual thalamic nuclei (Winer & Larue, 1996) that could allow pentobarbital to affect burst spiking of TRN auditory and visual cells in different manners (Mehta & Ticku, 1999; Wan *et al.*, 2003). The variations of burst spiking associated with the topographies of cell body and terminal field locations in the present and previous results seem to signify the presence of anatomical substrate rather than the influence of anesthesia for the properties of burst spiking. As such, pentobarbital is less likely to characterize the properties of burst spiking in the present and previous studies, suggesting the possibility that the distinctions in burst spiking between the lemniscal and non-lemniscal systems could be recognized in the TRN as well as thalamic nuclei (Ramcharan *et al.*, 2005) of non-anesthetized animals. Further studies of non-anesthetized animals are needed to test this possibility.

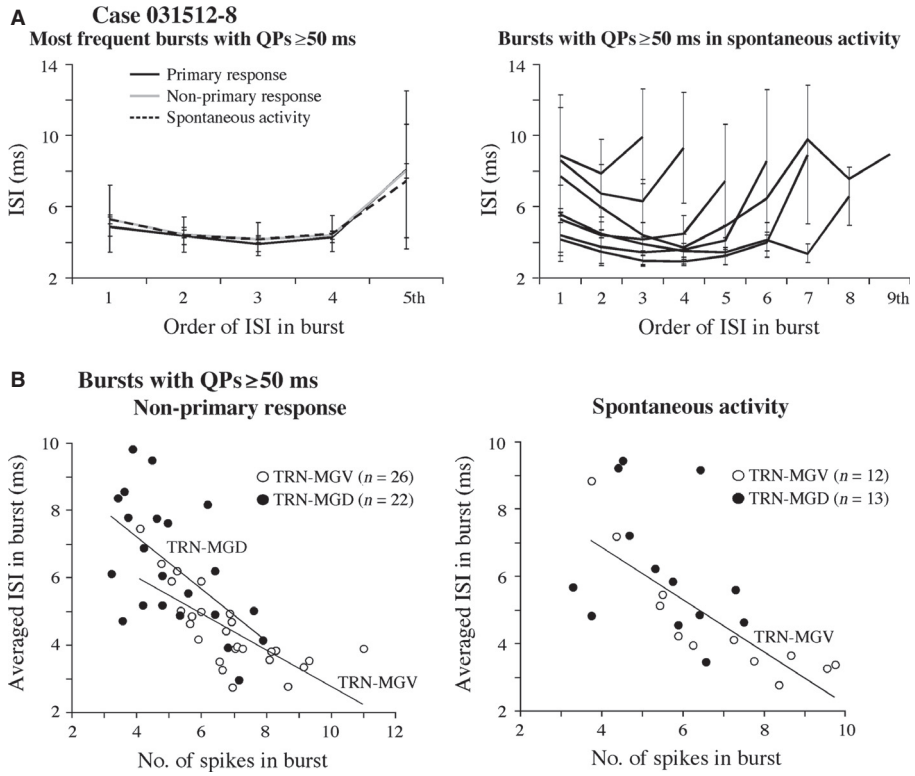

FIG. 10. Features of burst spiking detected on the basis of a longer maximum ISI (20 ms) and a shorter minimum preceding QP (50 ms). (A) Similar intra-burst ISI profiles (an initial progressive decrease followed by a progressive increase of length) were observed in bursts preceded by QPs ≥ 50 ms across primary, non-primary auditory responses and spontaneous activity (left graph). The profiles of intra-burst ISIs were consistently observed irrespective of the number of spikes composing a burst in spontaneous activity (right graph). (B) Bursts preceded by QPs ≥ 50 ms in non-primary auditory response (left graph) in the TRN-MGV cell group (white circles) were composed of larger numbers of spikes with shorter averaged ISIs as compared with those in the TRN-MGD cell group (black circles). There was no difference in the slope of the regression line between the TRN-MGV and TRN-MGD cell groups (continuous lines in left graph). In the TRN-MGV cell group the numbers of spikes composing a burst correlated with averaged intra-burst ISIs (continuous line in right graph) in bursts preceded by QPs ≥ 50 ms in spontaneous activity. There were no differences in the features of burst spiking between the TRN-MGV and TRN-MGD cell groups in spontaneous activity.

Anatomically structured features of burst spiking

One might raise a concern about the possibility that the interpretation of the previous (Kimura *et al.*, 2012b) and present results is confounded with changes of brain state due to fluctuations in the levels of anesthesia and/or differences in the efficacy of sensory stimulation for evoking burst spiking. However, the association between burst spiking and anatomical organization observed across sensory modalities is thought to rule out this possibility. Fluctuations in the levels of anesthesia across recordings would not allow us to observe the distinctions and variations in the features of burst spiking that are associated with anatomical organization in a similar manner across sensory modalities. Differences in the efficacy of sensory stimulation are considered negligible for visual modality because the distinctions and variations are recognized in spontaneous activity (Kimura *et al.*, 2012b). Although the distinctions in burst spiking between the TRN-MGV and TRN-MGD cell groups were not obvious in spontaneous activity, the correlation between burst spiking in spontaneous activity and anatomical organization (Figs 8E and F) suggests that differences in the efficacy of sound stimulation are unlikely to make a distinction in burst spiking. For the present study, tonotopy-based differential cell activation could be another concern. Tonotopy is considered organized primarily along the dorsoventral neural axis in the rat MG and TRN (Bordi & LeDoux, 1994; Kimura *et al.*, 2005, 2009, 2012a). In the results, the features of burst spiking did not change along the dorsoventral neural axis, however. Rather, the variations of burst spiking were observed along the rostrocaudal neural axis and marked in the TRN-MGD cell group that is supposed to receive thalamic inputs primarily from the MGD where tonotopy is obscure. Thus, tonotopy-based differential cell activation is unlikely to contribute to the present results. Taken together, the features of burst spiking associated with afferent (cell body) and efferent (terminal field) connections of the TRN are thought to reflect anatomically structured functional properties of the TRN.

The present study confirms the previous finding that TRN cells send axonal projections to the MGV topographic along the rostrocaudal, dorsoventral and mediolateral neural axes (Kimura *et al.*, 2007) and for the first time indicates the topography of projections to the MGD along the rostrocaudal neural axis. The features of burst spiking correlated with the rostrocaudal locations of cell bodies in both the TRN-MGV and TRN-MGD cell groups and thereby correlated with the rostrocaudal locations of terminal fields in the MGV and MGD. These findings raise the possibility that afferent and efferent connections of the TRN are organized in a way that allows the TRN to impose graded impacts of burst spiking on thalamic information processing along the rostrocaudal neural axis. The MGV of the rat has response properties and anatomical connectivities regionally differentiated along the rostrocaudal neural axis (Kimura *et al.*, 2003, 2005, 2012a; Donishi *et al.*, 2011). The correlation between intra-burst ISIs in auditory response and the locations

TABLE 3. Comparisons in the features of cell activity (ISIs in burst < 20 ms) between TRN-MGV and TRN-MGD cell groups; values are mean ± SD

	TRN-MGV	TRN-MGD
Auditory response		
Primary and non-primary responses		
No. of events (/s)	2.57 ± 1.61	2.05 ± 1.08
% of burst spiking*	94.1 ± 7.6	78.5 ± 21.3
No. of spikes in burst*	6.91 ± 1.60	5.04 ± 1.36
Averaged ISI in burst (ms)*	4.41 ± 1.16	6.37 ± 1.95
First ISI in burst (ms)*	4.96 ± 1.48	7.32 ± 2.57
Events with QPs ≥ 50 ms (non-primary response)		
No. of events (/s)	2.08 ± 1.31	1.56 ± 0.78
No. of spikes (/s)*	13.14 ± 7.86	6.71 ± 4.03
% of burst spiking*	96.5 ± 5.8	84.2 ± 18.1
No. of spikes in burst*	6.87 ± 1.58	5.14 ± 1.43
Averaged ISI in burst (ms)*	4.44 ± 1.17	6.32 ± 1.88
First ISI in burst (ms)*	4.87 ± 1.39	7.30 ± 2.51
Spontaneous activity		
All events		
No. of events (/s)	1.09 ± 0.93	1.29 ± 0.81
% of burst spiking	89.4 ± 17.5	77.0 ± 24.3
No. of spikes in burst	6.86 ± 2.00	5.42 ± 1.29
Averaged ISI in burst (ms)	4.63 ± 1.81	6.31 ± 2.06
First ISI in burst (ms)	5.01 ± 2.07	7.57 ± 3.04
Events with QPs ≥ 50 ms		
No. of events (/s)	0.98 ± 0.79	1.04 ± 0.58
No. of spikes (/s)	5.15 ± 3.58	4.50 ± 2.55
% of burst spiking	92.6 ± 14.9	82.3 ± 22.2
No. of spikes in burst	6.87 ± 1.98	5.52 ± 1.32
Averaged ISI in burst (ms)	4.62 ± 1.79	6.20 ± 1.97
First ISI in burst (ms)	4.98 ± 2.02	7.52 ± 3.10

QP, quiescent period; *$P < 0.05$, corrected for multiple comparisons.

of cell bodies and terminal fields in the TRN-MGV cell group, although fairly weak, may contribute to the rostrocaudal gradient of response properties of MGV cells, as with the rostrocaudally graded density of GABA cells in the MGV of the cat (Rodrigues-Dagaeff *et al.*, 1989; Rouiller *et al.*, 1990). The correlation in the TRN-MGD cell group, which, although limited to the numbers of spikes composing a burst, was consistently observed in auditory response and spontaneous activity, appears strong as compared with the correlation in the TRN-MGV cell group. Of note is that there seems to be an interesting anatomical coincidence between this finding and a recent report that has documented regional differences in the intensity of stimulus-specific adaptation (SSA) in the MGV and MGD (Antunes *et al.*, 2010). TRN-MGV and TRN-MGD cells with the distinct features of burst spiking and recurrent activation (non-primary response) may provide differential influences on auditory change detection of MGV and MGD cells (Yu *et al.*, 2009), which could be represented as distinct intensities of SSA observed in the MGV and MGD (Antunes *et al.*, 2010). Lower intensities of SSA are observed in the whole MGV and the rostral MGD where TRN cells with higher levels of burst spiking send axonal projections, while higher intensities of SSA are observed in the caudal MGD where TRN cells with lower levels of burst spiking send axonal projections. It could be possible to assume that the strong correlation in the TRN-MGD cell group may provide graded influences on thalamic cell activity resulting in the rostrocaudal gradient of SSA intensity inside the MGD while the weak correlation in the TRN-MGV cell group may fail to provide differential influences resulting in the absence of a regional gradient inside the MGV (Antunes *et al.*, 2010).

In both auditory and visual modalities, the features of burst spiking in spontaneous activity correlate with the rostrocaudal locations of cell bodies, and the rostral and caudal domains of the TRN are allocated to the two types of TRN cells projecting to first- and higher-order thalamic nuclei (Kimura *et al.*, 2012b). As such, auditory and visual systems seem to adopt a common structural arrangement of burst spiking for the TRN to serve distinct modulations of lemniscal and non-lemniscal sensory processing. There may be an anatomically structured functional matrix other than those for tonotopy- and retinotopy-based processing (Kimura *et al.*, 2005, 2007, 2009, 2012a; Fitzgibbon *et al.*, 2007; Cotillon-Williams *et al.*, 2008). Questions then arise. Does the rostrocaudal gradient of burst spiking features extend to the further rostral TRN that contains somatosensory cells (Shosaku & Sumitomo, 1983)? Do somatosensory cells projecting to first- and higher-order thalamic nuclei have distinct cell activities and distributions in the TRN? Further studies addressing these questions are needed to clarify how the sensory sectors of the TRN are organized as a whole to modulate sensory processing in lemniscal and non-lemniscal thalamocortical loop connections that converge on the TRN (Pinault, 2004; Kimura *et al.*, 2012a).

Functional implications

The TRN is known to decisively modulate thalamic cell activity (French *et al.*, 1985; Halassa *et al.*, 2011). MGV and MGD cells have similar intrinsic properties in slice preparations (Bartlett & Smith, 1999). Therefore, TRN cells with distinct features of burst spiking are thought to mold MGV and MGD cell activities into different types. TRN cells with higher levels of burst spiking are assumed to impose stronger inhibition on thalamic cells (Kim *et al.*, 1997), which would condition MGV cells to more frequently discharge in burst than MGD cells. This assumption, however, contradicts low and high levels of burst spiking observed in MGV and MGD cell activities (primary response) directly driven by sound stimulation (He & Hu, 2002). In primary response, cortical (Wolfart *et al.*, 2005) and/or neuromodulator inputs (Varela & Sherman, 2007, 2009) rather than TRN inputs may have significant influences for conditioning MGV and MGD cells to show distinct activities in response to tectal excitatory and/or inhibitory inputs (Bartlett & Smith, 1999). On the other hand, the TRN may provide a significant impact for molding discharge patterns in non-primary response. A notable finding is that MGV cells have a clear tendency to show single spikes in primary response and bursts in repeatedly evoked non-primary responses (Kimura *et al.*, 2009). TRN-MGV cells with higher levels of burst spiking could provide potent inhibition, which would effectively condition MGV cells to discharge in burst in non-primary response.

Sound stimulation sustainably attenuated the intensities of burst spiking of TRN-MGV cells in terms of the number and density of spikes in a burst, whereas it transiently attenuated those of TRN-MGD cells. Sustained and transient alterations of burst spiking are also observed in TRN visual cells projecting to the DLG and LP following light stimulation (Kimura *et al.*, 2012b). Interestingly, the alterations of burst spiking in visual cells are enhancement. The difference in the direction of alteration may be related to possible distinctions in the properties of thalamocortical loop circuitries inherent to auditory and visual modalities, such as the distinct distributions of Typical- and Atypical-burst types of cells in the visual and auditory domains of the TRN (Lee *et al.*, 2007) and the distinct densities of inhibitory interneurons in visual and auditory thalamic nuclei (Winer & Larue, 1996). Alternatively, the differential impacts of

light and sound stimuli used for cell activation could be a cause of the difference. Apart from the difference in the direction of alteration, the sustained alteration could allow TRN auditory and visual cells projecting to first-order thalamic nuclei to incorporate the impacts of sensory inputs into recurrent activation of thalamocortical loop circuitry for temporally integrated sensory processing. On the other hand, TRN auditory and visual cells projecting to higher-order thalamic nuclei are less likely to incorporate the impacts of sensory inputs into recurrent activation, but the transient alteration of burst spiking could highlight the moment of sensory activation for attentive sensory processing. Together with these distinctions, the synergy between thalamic and TRN cell activities with their contrasting features of burst spiking may compose distinct information processing and attentional gating functions of the lemniscal and non-lemniscal sensory systems.

Acknowledgements

We are grateful to T. Tsujinaka for her assistance with histology. This work was supported by a Grant-in-Aid for Scientific Research (C) from Japan Society for the Promotion of Science (23500397) to A.K. The authors declare no competing financial interests.

Abbreviations

DLG, dorsal lateral geniculate nucleus; ISI, inter-spike interval; LP, lateral posterior nucleus; LTS, low-threshold calcium spike; MG, medial geniculate nucleus; MGD, dorsal division of the medial geniculate nucleus; MGM, medial division of the medial geniculate nucleus; MGV, ventral division of the medial geniculate nucleus; QP, quiescent period; SG, suprageniculate nucleus; SSA, stimulus-specific adaptation; TRN, thalamic reticular nucleus.

References

Antunes, F.M., Nelken, I., Covey, E. & Malmierca, M.S. (2010) Stimulus-specific adaptation in the auditory thalamus of the anesthetized rat. *PLoS One*, **5**, e14071.

Bartlett, E.L. & Smith, P.H. (1999) Anatomic, intrinsic, and synaptic properties of dorsal and ventral divisions in rat medial geniculate body. *J. Neurophysiol.*, **81**, 1999–2016.

Bordi, F. & LeDoux, J.E. (1994) Response properties of single units in areas of rat auditory thalamus that project to the amygdala. *Exp. Brain Res.*, **98**, 261–274.

Cappe, C., Rouiller, E.M. & Barone, P. (2009) Multisensory anatomical pathways. *Hearing Res.*, **258**, 28–36.

Cotillon-Williams, N. & Edeline, J.-M. (2003) Evoked oscillations in the thalamo-corical auditory system are present in anesthetized but not in unanesthetized rats. *J. Neurophysiol.*, **89**, 1968–1984.

Cotillon-Williams, N., Huetz, C., Hennevin, E. & Edeline, J.-M. (2008) Tonotopic control of auditory thalamus frequency tuning by reticular thalamic neurons. *J. Neurophysiol.*, **99**, 1137–1151.

Domich, L., Oakson, G. & Steriade, M. (1986) Thalamic burst patterns in the naturally sleeping cat: a comparison between cortically projecting and reticularis neurons. *JPN J. Physiol.*, **379**, 429–449.

Donishi, T., Kimura, A., Imbe, H., Yokoi, I. & Kaneoke, Y. (2011) Subthreshold cross-modal sensory interaction in the thalamus: lemniscal auditory response in the medial geniculate nucleus is modulated by somatosensory stimulation. *Neuroscience*, **174**, 200–215.

Fitzgibbon, T., Szmajda, B.A. & Martin, P.R. (2007) First order connections of the visual sector of the thalamic reticular nucleus. *Visual Neurosci.*, **24**, 857–874.

French, C.R., Sefton, A.J. & Mackay-Sim, A. (1985) The inhibitory role of the visually responsive region of the thalamic reticular nucleus in the rat. *Exp. Brain Res.*, **57**, 471–479.

Halassa, M.M., Siegle, J., Ritt, J.T., Ting, J.T., Feng, G. & Moore, C.I. (2011) Selective optical drive of thalamic reticular nucleus generates thalamic bursts and cortical spindles. *Nat. Neurosci.*, **14**, 1118–1120.

Hartings, J.A., Temereanca, S. & Simons, D.J. (2003) State-dependent processing of sensory stimuli by thalamic reticular neurons. *J. Neurosci.*, **23**, 5264–5271.

He, J. & Hu, B. (2002) Differential distribution of burst and single-spike responses in auditory thalamus. *J. Neurophysiol.*, **88**, 2152–2156.

Horikawa, K. & Armstrong, W.E. (1988) A versatile means of intracellular labeling: injection of biocytin and its detection with avidin conjugates. *J. Neurosci. Meth.*, **25**, 1–25.

Huguenard, J.R. & McCormick, D.A. (2007) Thalamic synchrony and dynamic regulation of global forebrain osciilations. *Trends Neurosci.*, **30**, 350–356.

Jones, E.G. (2009) Synchrony in the interconnected circuitry of the thalamus and cerebral cortex. *Ann. NY Acad. Sci.*, **1157**, 10–23.

Kim, U., Sanchez-Vives, M.V. & McCormick, D.A. (1997) Functional dynamics of GABAergic inhibition in the thalamus. *Science*, **278**, 130–134.

Kimura, A. (2014) Diverse subthreshold cross-modal sensory interactions in the thalamic reticular nucleus: implications for new pathways of cross-modal attentional gating function. *Eur. J. Neurosci.*, **39**, 1405–1418.

Kimura, A., Donishi, T., Sakoda, T., Hazama, M. & Tamai, Y. (2003) Auditory thalamic nuclei projections to the temporal cortex in the rat. *Neuroscience*, **117**, 1003–1016.

Kimura, A., Donishi, T., Okamoto, K. & Tamai, Y. (2005) Topography of projections from the primary and non-primary auditory cortical areas to the medial geniculate body and thalamic reticular nucleus. *Neuroscience*, **135**, 1325–1342.

Kimura, A., Imbe, H., Donishi, T. & Tamai, Y. (2007) Axonal projections of single auditory neurons in the thalamic reticular nucleus: implications for tonotopy-related gating function and cross-modal modulation. *Eur. J. Neurosci.*, **26**, 3524–3535.

Kimura, A., Imbe, H. & Donishi, T. (2009) Axonal projections of auditory cells with short and long response latencies in the medial geniculate nucleus: distinct topographies in the connection with the thalamic reticular nucleus. *Eur. J. Neurosci.*, **30**, 783–799.

Kimura, A., Yokoi, I., Imbe, H., Donishi, T. & Kaneoke, Y. (2012a) Auditory thalamic reticular nucleus of the rat: anatomical nodes for modulation of auditory and cross-modal sensory processing in the loop connectivity between the cortex and thalamus. *J. Comp. Neurol.*, **520**, 1457–1480.

Kimura, A., Yokoi, I., Imbe, H., Donishi, T. & Kaneoke, Y. (2012b) Distinctions in burst spiking between thalamic reticular nucleus cells projecting to the dorsal lateral geniculate and lateral posterior nuclei in the anesthetized rat. *Neuroscience*, **226**, 208–226.

Komura, Y., Tamura, R., Uwano, T., Nishijo, H., Kaga, K. & Ono, T. (2001) Retrospective and prospective coding for predicted reward in the sensory thalamus. *Nature*, **412**, 546–549.

Landisman, C.E., Long, M.A., Beierlein, M., Deans, M.R., Paul, D.L. & Connors, B.W. (2002) Electrical synapses in the thalamic reticular nucleus. *J. Neurosci.*, **22**, 1002–1009.

Lee, S.-H., Govindaiah, G. & Cox, C.L. (2007) Heterogeneity of firing properties among rat thalamic reticular neurons. *JPN J. Physiol.*, **582**, 195–208.

Llinás, R.R. & Steriade, M. (2006) Bursting of thalamic neurons and states of vigilance. *J. Neurophysiol.*, **95**, 3297–3308.

Lu, S.-M., Guido, W. & Sherman, S.M. (1992) Effects of membrane voltage on receptive field properties of lateral geniculate neurons in the cat: contributions of the low-threshold Ca^{2+} conductance. *J. Neurophysiol.*, **68**, 2185–2198.

Massaux, A. & Edeline, J.-M. (2003) Bursts in the medial geniculate body: a comparison between anesthetized and unaesthetized states in guinea pig. *Exp. Brain Res.*, **153**, 573–578.

Massaux, A., Dutrieux, G., Cotillon-Williams, N., Manunta, Y. & Edeline, J.-M. (2004) Auditory thalamus bursts in anesthetized and non-anesthetized states: contribution to functional properties. *J. Neurophysiol.*, **91**, 2117–2134.

Mehta, A.K. & Ticku, M.K. (1999) An update on GABA receptors. *Brain Res. Rev.*, **29**, 196–217.

Paxinos, G. & Watson, C. (1997) *The Rat Brain in Stereotaxic Coordinates*. Academic Press, San Diego.

Pinault, D. (1996) A novel single-cell staining procedure performed in vivo under electrophysiological control: morpho-functional features of juxtacellularly labeled thalamic cells and other central neurons with biocytin or Neurobiotin. *J. Neurosci. Meth.*, **65**, 113–136.

Pinault, D. (2003) Cellular interactions in the rat somatosensory thalamocortical systems during normal and epileptic 5–9 Hz oscillations. *JPN J. Physiol.*, **552**, 881–905.

Pinault, D. (2004) The thalamic reticular nucleus: structure, function and concept. *Brain Res. Rev.*, **46**, 1–31.

Ramcharan, E.J., Gnadt, J.W. & Sherman, S.M. (2005) High-order thalamic relays burst more than first-order relays. *Proc. Natl. Acad. Sci. USA*, **102**, 12236–12241.

Rodrigues-Dagaeff, C., Simm, G., De Ribaupierre, Y., Villa, A., De Ribaupierre, F. & Rouiller, E.M. (1989) Functional organization of the ventral division of the medial geniculate body of the cat: evidence for a rostrocaudal gradient of response properties and cortical projections. *Hearing Res.*, **39**, 103–125.

Rouiller, E.M., Capt, M., Hornung, J.P. & Streit, P. (1990) Correlation between regional changes in the distributions of GABA-containing neurons and unit response properties in the medial geniculate body of the cat. *Hearing Res.*, **49**, 249–258.

Sherman, S.M. (2012) Thalamocortical interactions. *Curr. Opin. Neurobiol.*, **22**, 575–579.

Shosaku, A. & Sumitomo, I. (1983) Auditory neurons in the rat thalamic reticular nucleus. *Exp. Brain Res.*, **49**, 432–442.

Shosaku, A., Kayama, Y., Sumitomo, I., Sugitani, M. & Iwama, K. (1989) Analysis of recurrent inhibitory circuit in rat thalamus: neurophysiology of the thalamic reticular nucleus. *Prog. Neurobiol.*, **32**, 77–102.

Sohal, V.S. & Huguenard, J.R. (2003) Inhibitory interactions control burst pattern and emergent network synchrony in reticular thalamus. *J. Neurosci.*, **23**, 8978–8988.

Steriade, M. (2006) Grouping of brain rhythms in corticothalamic systems. *Neuroscience*, **137**, 1087–1106.

Steriade, M., Domich, L., Oakson, G. & Deschênes, M. (1987) The deafferented reticular thalamic nucleus generates spindle rhythmicity. *J. Neurophysiol.*, **57**, 260–273.

Sumitomo, I., Takahashi, Y., Kayama, Y. & Ogawa, T. (1989) Burst discharges of thalamic reticular neurons: an intracellular analysis in anesthetized rats. *Brain Res.*, **482**, 34–41.

Sun, Y.-G., Wu, C.-S., Renger, J.J., Uebele, V.N., Lu, H.-C. & Beierlein, M. (2012) GABAergic synaptic transmission triggers action potentials in thalamic reticular nucleus neurons. *J. Neurosci.*, **32**, 7782–7790.

Swadlow, H.A. & Gusev, A.G. (2001) The impact of 'bursting' thalamic impulses at a neocortical synapse. *Nat. Neurosci.*, **4**, 402–408.

Varela, C. & Sherman, S.M. (2007) Differences in response to muscarinic activation between first and higher order thalamic relays. *J. Neurophysiol.*, **98**, 3538–3547.

Varela, C. & Sherman, S.M. (2009) Differences in response to serotonergic activation between first and higher order thalamic nuclei. *Cereb. Cortex*, **19**, 1776–1786.

Wan, X., Mathers, A. & Puil, E. (2003) Pentobarbital modulates intrinsic and GABA-receptor conductances in thalamocortical inhibition. *Neuroscience*, **121**, 947–958.

Wei, H., Bonjean, M., Petry, H.M., Sejnowski, T.J. & Bickford, M.E. (2011) Thalamic burst firing propensity: a comparison of the dorsal lateral geniculate and pulvinar nuclei in the three shrew. *J. Neurosci.*, **31**, 17287–17299.

Winer, J.A. & Larue, D.T. (1996) Evolution of GABAergic circuitry in the mammalian medial geniculate body. *Proc. Natl. Acad. Sci. USA*, **93**, 3083–3087.

Wolfart, J., Debay, D., Le Masson, G., Destexhe, A. & Thierry, B. (2005) Synaptic background activity controls spike transfer from thalamus to cortex. *Nat. Neurosci.*, **8**, 1760–1767.

Yu, X.-J., Xu, X.-X., He, S. & He, J. (2009) Change detection by thalamic reticular neurons. *Nat. Neurosci.*, **12**, 1165–1171.

Zaman, T., Lee, K., Park, C., Paydar, A., Choi, J.H., Cheong, E., Lee, C.J. & Shin, H.-S. (2011) Cav2.3 channels are critical for oscillatory burst discharges in the reticular thalamus and absence epilepsy. *Neuron*, **70**, 95–108.